



**UNIVERSIDAD DE INVESTIGACIÓN DE TECNOLOGÍA
EXPERIMENTAL YACHAY**

Escuela de Ciencias Biológicas e Ingeniería

TÍTULO: “Cellulose-based microspheres as a possible method for drug release in the treatment of leishmaniasis disease”

Trabajo de integración curricular presentado como requisito para la obtención del título de Ingeniería Biomédica

Autor:

Guagchinga Moreno Genesis Yulisa

Tutor:

Ph.D. Alexis Frank

Co-tutor:

MSC. Santamaría Javier

Urququí, enero del 2022

SECRETARÍA GENERAL
(Vicerrectorado Académico/Cancillería)
ESCUELA DE CIENCIAS BIOLÓGICAS E INGENIERÍA
CARRERA DE BIOMEDICINA
ACTA DE DEFENSA No. UITEY-BIO-2022-00001-AD

A los 7 días del mes de enero de 2022, a las 18:00 horas, de manera virtual mediante videoconferencia, y ante el Tribunal Calificador, integrado por los docentes:

Presidente Tribunal de Defensa	Dr. SANTIAGO VISPO, NELSON FRANCISCO , Ph.D.
Miembro No Tutor	Dra. LIRA VERGARA RENE CONSTANZA , Ph.D.
Tutor	Dr. ALEXIS FRANK , Ph.D.

El(la) señor(ita) estudiante **GUAGCHINGA MORENO, GENESIS YULISA**, con cédula de identidad No. **0550054704**, de la **ESCUELA DE CIENCIAS BIOLÓGICAS E INGENIERÍA**, de la Carrera de **BIOMEDICINA**, aprobada por el Consejo de Educación Superior (CES), mediante Resolución **RPC-SO-43-No.496-2014**, realiza a través de videoconferencia, la sustentación de su trabajo de titulación denominado: **Cellulose-based microspheres as a possible method for drug release in the treatment of leishmaniasis disease.** , previa a la obtención del título de **INGENIERO/A BIOMÉDICO/A**.

El citado trabajo de titulación, fue debidamente aprobado por el(los) docente(s):

Tutor	Dr. ALEXIS FRANK , Ph.D.
--------------	--------------------------

Y recibió las observaciones de los otros miembros del Tribunal Calificador, las mismas que han sido incorporadas por el(la) estudiante.

Previamente cumplidos los requisitos legales y reglamentarios, el trabajo de titulación fue sustentado por el(la) estudiante y examinado por los miembros del Tribunal Calificador. Escuchada la sustentación del trabajo de titulación a través de videoconferencia, que integró la exposición de el(la) estudiante sobre el contenido de la misma y las preguntas formuladas por los miembros del Tribunal, se califica la sustentación del trabajo de titulación con las siguientes calificaciones:

Tipo	Docente	Calificación
Miembro Tribunal De Defensa	Dra. LIRA VERGARA RENE CONSTANZA , Ph.D.	10,0
Tutor	Dr. ALEXIS FRANK , Ph.D.	10,0
Presidente Tribunal De Defensa	Dr. SANTIAGO VISPO, NELSON FRANCISCO , Ph.D.	10,0


Lo que da un promedio de: **10 (Diez punto Cero)**, sobre 10 (diez), equivalente a: **APROBADO**

Para constancia de lo actuado, firman los miembros del Tribunal Calificador, el/la estudiante y el/la secretario ad-hoc.

Certifico que *en cumplimiento del Decreto Ejecutivo 1017 de 16 de marzo de 2020, la defensa de trabajo de titulación (o examen de grado modalidad teórico práctica) se realizó vía virtual, por lo que las firmas de los miembros del Tribunal de Defensa de Grado, constan en forma digital.*

GUAGCHINGA MORENO, GENESIS YULISA
Estudiante

Dr. SANTIAGO  **NELSON FRANCISCO , Ph.D.**
Presidente Tribunal de Defensa

Dr. ALEXIS FRANK , Ph.D.
Tutor  **FRANK ALEXIS**



Firmado electrónicamente por:
RENE CONSTANZA
LIRA VERGARA

Dra. LIRA VERGARA RENE CONSTANZA , Ph.D.
Miembro No Tutor



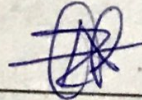
Firmado electrónicamente por:
KARLA
ESTEFANIA
ALARCON FELIX

ALARCON FELIX, KARLA ESTEFANIA
Secretario Ad-hoc

AUTORÍA

Yo, Genesis Yulisa Guagchinga Moreno, con cédula de identidad 0550054704, declaro que las ideas, juicios, valoraciones, interpretaciones, consultas bibliográficas, definiciones y conceptualizaciones expuestas en el presente trabajo; así cómo, los procedimientos y herramientas utilizadas en la investigación, son de absoluta responsabilidad de el/la autora (a) del trabajo de integración curricular. Así mismo, me acojo a los reglamentos internos de la Universidad de Investigación de Tecnología Experimental Yachay.

Urququí, enero del 2022.

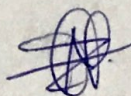


Genesis Yulisa Guagchinga Moreno
CI: 0550054704

AUTORIZACIÓN DE PUBLICACIÓN

Yo, Genesis Yulisa Guagchinga Moreno, con cédula de identidad 0550054704, cedo a la Universidad de Investigación de Tecnología Experimental Yachay, los derechos de publicación de la presente obra, sin que deba haber un reconocimiento económico por este concepto. Declaro además que el texto del presente trabajo de titulación no podrá ser cedido a ninguna empresa editorial para su publicación u otros fines, sin contar previamente con la autorización escrita de la Universidad. Asimismo, autorizo a la Universidad que realice la digitalización y publicación de este trabajo de integración curricular en el repositorio virtual, de conformidad a lo dispuesto en el Art. 144 de la Ley Orgánica de Educación Superior.

Urququí, enero del 2022.



Genesis Yulisa Guagchinga Moreno

CI: 0550054704

DEDICATORIA

Con mucho amor para mis padres Luis y Susana, y mis hermanos Polo y Vicky, quienes con su ejemplo y enseñanzas me han inspirado a cumplir mis sueños, y me han apoyado en los momentos de adversidad.

A mí Alma Máter, Universidad Yachay Tech, y a sus docentes quienes me han brindado las herramientas necesarias para culminar con éxito mis estudios universitarios, y me han inculcado la pasión por la investigación.

A mi mentor, y supervisor, Frank Alexis PhD, quien me proporcionó los conocimientos necesarios para desarrollar este trabajo investigativo.

A mis amigos, con quienes compartí la vida universitaria, siempre añoraré los momentos que compartimos juntos.

Genesis Yulisa Guagchinga Moreno

AGRADECIMIENTOS

A Dios, por la salud y la vida.

A mis padres Luis y Susana y a mis hermanos Polo y Vicky, por su amor incondicional. Siempre estaré agradecida por la educación que me supieron brindar y todas las enseñanzas que me han dado.

A la Universidad Yachay Tech, en especial a la Escuela de Ciencias Biológicas e Ingeniería, por permitirme hacer uso de cada uno de sus laboratorios para la realización de este trabajo investigativo.

Al Instituto de Investigación en Zoonosis (CIZ) – Quito, por asesorarme y permitirme hacer uso sus instalaciones.

A Frank Alexis PhD, por su tiempo y dedicación para el desarrollo de este proyecto de grado.

A todas las personas que me apoyaron incondicionalmente en la realización de este trabajo, en especial a los técnicos de los laboratorios de biología, química y geología. Además, agradecimiento a los docentes de la Escuela de Química.

Genesis Yulisa Guagchinga Moreno

RESUMEN

La leishmaniasis es una enfermedad infecciosa y parasitaria causada por un parásito protozoario del género *Leishmania*. Se transmite a los humanos a través de la picadura de hembras infectadas de flebótomos, principalmente *Phlebotomus* y *Lutzomyia*. Hay tres formas principales en que se presenta la enfermedad: leishmaniasis visceral (LV) o kala-azar, leishmaniasis cutánea (LC) y leishmaniasis mucocutánea (LM). La incidencia de personas enfermas con leishmaniasis es mundial, por ejemplo, anualmente se reportan entre 600000 a 1 millón casos nuevos con LC, y entre 50000 a 90000 casos de LV. Por otra parte, en Ecuador existe alta incidencia de LC y LM representando un problema de salud pública. De hecho, en el año 2018 se registraron 1268 casos de personas enfermas. Y para el año 2019, se reportó que en 22 de las 24 provincias del territorio ecuatoriano se presentaron casos, siendo Pichincha la provincia con mayor número de contagiados (144). En lo referente a tratamientos contra la leishmaniasis, los medicamentos más comunes utilizados son miltefosina, antimoniales (Sb^v) y amphotericin b (AmB). Sin embargo, estos medicamentos solo pueden administrarse por vía oral (píldoras) o tópicos (ungüentos), por lo que es necesario desarrollar un nuevo e innovador sistema a base de compuestos naturales como es la celulosa para la administración de este tipo de fármacos y que sea amigable con el paciente. De hecho, hoy en día, los biomateriales basados en celulosa están siendo utilizados en la industria farmacológica debido a su capacidad para la liberación de medicamentos. De esta manera, el objetivo de este trabajo es desarrollar un nuevo método de liberación de fármacos para tratar la enfermedad de la leishmaniasis utilizando perlas a base de celulosa, las cuales son sintetizadas de celulosa obtenida de fuentes naturales a través de diferentes procesos químicos y físicos. Es así que, la celulosa es caracterizada mediante espectroscopia infrarroja por transformada de Fourier (FTIR) y cristalografía de rayos X (XRD). Además, la caracterización de las perlas a base

de celulosa se obtiene mediante microscopía electrónica de barrido (SEM) y mediante el uso de un estereoscopio. Por otra parte, se determinó el perfil de liberación de fármacos de las perlas.

Palabras clave:

Perlas a base de celulosa, leishmaniasis, liberación de fármacos, biomaterial

ABSTRACT

Leishmaniasis is an infectious and parasitic disease caused by a protozoan parasite of the genus *Leishmania*. It is transmitted to humans through the bite of infected female sandflies, mainly *Phlebotomus* and *Lutzomyia*. There are three main forms in which the disease appears: visceral leishmaniasis (VL) or kala-azar, cutaneous leishmaniasis (CL), and mucocutaneous leishmaniasis (ML). The incidence of sick people with leishmaniasis is worldwide; for example, annually, between 600 000 to 1 million new cases with CL are reported, and between 50 000 to 90 000 cases of VL. On the other hand, there is a high incidence of CL and ML in Ecuador, representing a public health problem. In fact, in 2018, 1 268 cases of sick people were registered. And for the year 2019, it was reported that there were cases in 22 of the 24 provinces of the Ecuadorian territory there were cases of leishmaniasis, with Pichincha being the province with the highest number of infected persons (144). For leishmaniasis treatments, the most common medications used are miltefosine, antimonials (Sb^v), and amphotericin b (AmB). However, these drugs can only be administered orally (pills) or topically (ointments), so it is necessary to develop a new and innovative system based on natural compounds such as cellulose for the administration of this type of drug which is patient friendly. In fact, today, cellulose-based biomaterials are being used in the pharmaceutical industry due to their ability to release drugs. In this way, this work aims to develop a new method of drug release to treat leishmaniasis disease using cellulose-based beads, which are synthesized from cellulose obtained from natural sources through different chemical and physical processes. Thus, cellulose is characterized by Fourier transform infrared spectroscopy (FTIR) and X-ray crystallography (XRD). Furthermore, the characterization of the cellulose-based beads is obtained by scanning electron microscopy (SEM) and by using a stereoscope. Moreover, the drug release profile of the beads was determined.

Key-words:

Cellulose-based beads, leishmaniasis, drug release, biomaterial

INDEX

1. INTRODUCTION – JUSTIFICATION	11
1.1. Leishmaniasis	11
1.2. Treatments and therapies against leishmaniasis	14
1.3. Cellulose as drug delivery	15
1.4. Beads-based cellulose	16
1.5. Methylene blue	17
2. PROBLEM STATEMENT	17
2.1. Relevance to Ecuador	17
3. HYPOTHESIS AND OBJECTIVES	18
3.1. Hypothesis	18
3.2. General objective	18
3.2.1. Specific objectives	19
4. METHODS	19
4.1. Materials	19
4.2. Cellulose fibers extraction	19
4.3. Synthesis of cellulose-based beads	20
4.4. Characterization	20
4.4.1. Cellulose fibers characterization	20
4.4.3. Drug profile release	21
4.5. Release Kinetics Analysis	22
5. RESULTS, INTERPRETATION, AND DISSCUSION	22
5.1. Cellulose fibers extraction	22
5.2. Cellulose fibers characterization	23
5.2.1. Fourier-transform infrared spectroscopy	23
5.2.2. X-Ray Diffraction	26
5.3. Cellulose beads synthesis	29
5.4. Cellulose beads characterization	33
5.4.1. Stereo Microscope	33
5.4.2. Scanning Electron Microscopy	34
5.4.3. X-Ray Nano tomograhy Analysis	36
5.5. Release profile	36
5.6. Kinetics Release Model	39
6. CONCLUSIONS AND RECOMMENDATIONS	42

7. REFERENCES	44
8. ANNEXES	47

List of Figures

Figure 1: The life cycle of Leishmania species (Esch & Petersen, 2013).	12
Figure 2: Cutaneous leishmaniasis on leg. (Christian & Coque, 2020)	14
Figure 3: Chemical structure of cellulose.(George & Sabapathi, 2015)	16
Figure 4: Cellulose fibers from (A) apple, (B) mango, (C) avocado, and (D) pear	23
Figure 5: FTIR analysis of apple cellulose fibers	24
Figure 6: FTIR analysis of mango cellulose fibers	25
Figure 7: FTIR analysis of avocado cellulose fibers	25
Figure 8: FTIR analysis of pear cellulose fibers	26
Figure 9: FTIR analysis of commercial cellulose fibers	26
Figure 10: X-Ray Diffraction of the apple cellulose fibers	27
Figure 11: X-Ray Diffraction of the mango cellulose fibers	28
Figure 12: X-Ray Diffraction of the avocado cellulose fibers.....	28
Figure 13: X-Ray Diffraction of the pear cellulose fibers	29
Figure 14: X-Ray Diffraction of the commercial cellulose fibers	29
Figure 15: Cellulose beads synthesized from apple to different CaCl ₂ concentrations (A)0.6 M, (B)0.8 M, (C)1 M, and (D)1.2 M	31
Figure 16: Cellulose beads synthesized from mango to different CaCl ₂ concentrations (A)0.6 M, (B)0.8 M, (C)1 M, and (D)1.2 M	31
Figure 17: Cellulose beads synthesized from commercial cellulose to different CaCl ₂ concentrations (A)0.6 M, (B)0.8 M, (C)1 M, and (D)1.2 M	32
Figure 18: Cellulose beads synthesized from avocado cellulose to different CaCl ₂ concentrations (A)0.6 M, (B) 0.8 M, and (C)1 M	32
Figure 19: Cellulose beads synthesized from pear cellulose to different CaCl ₂ concentrations (A)0.6 M, (B)0.8 M, and (C)1 M	32
Figure 20: Dried apple cellulose bead prepared at 1 M CaCl ₂ solution under a stereo microscope at 3.2x	33
Figure 21: Dried mango cellulose bead prepared at 1 M CaCl ₂ solution under a stereo microscope at 3.2x.....	34
Figure 22: Dried commercial cellulose bead prepared at 1 M CaCl ₂ solution under a stereo microscope at 3.2x.....	34
Figure 23: SEM analysis from apple cellulose beads	35
Figure 24: SEM analysis from mango cellulose beads.	35
Figure 25: SEM analysis from commercial cellulose beads.	35
Figure 26: X-Ray Nanotomography analysis from cellulose beads. (A) apple bead, and (B) commercial bead.....	36
Figure 27: Methylene blue calibration curve	37
Figure 28: Methylene blue solution and cellulose beads	38
Figure 29: Percentage of methylene blue release from beads vs. time	38
Figure 30: First Order drug release model from apple, mango and commercial cellulose	41
Figure 31: Zero Order drug release model from apple, mango and commercial cellulose	53
Figure 32: Higuchi model from apple, mango and commercial cellulose	53

Figure 33: Hixson Model from apple, mango and commercial cellulose	54
Figure 34: Korsmeyer-Peppas Model from apple, mango and commercial cellulose	54

List of Tables

Table 1: Leishmania species distribution by ecological region in Ecuador	14
Table 2: Materials	19
Table 3: Absorption band peaks from cellulose fibers	24
Table 4: Cellulose crystallinity Index	27
Table 5: Results of cellulose beads synthesis from different cellulose fibers	30
Table 6: Size of cellulose beads	33
Table 7: Results of methylene blue release from cellulose beads	38

List of Schemes

Scheme 1: Process to cellulose beads synthesis	20
Scheme 2: Encapsulation of methylene blue in the cellulose beads	22

List of Equations

Equation 1: Crystallinity Index	27
Equation 2: First order kinetic equation	40

1. INTRODUCTION – JUSTIFICATION

1.1. Leishmaniasis

Leishmaniasis is a neglected disease of the poor caused by a parasitic protozoan called *Leishmania*. It is transmitted to humans through bites of infected female sandflies mainly *Phlebotomus* and *Lutzomyia* (Europe, Northern Africa, the Middle East, Asia, and part of South America). (Torres-Guerrero et al., 2017; World Health Organization, 2021) There are more than 20 different *Leishmania* species, and there are more than 90 parasite species that transmit *Leishmania*, and humans are natural reservoirs of *Leishmania* parasites. The leishmaniasis incidence and distribution depend on the transmission sites, parasite species characteristics, sandflies characteristics, previous and current exposition of humans to the parasite, and human behavior. (World Health Organization, 2021)

On the other hand, the life cycle of *Leishmania* involves a mammalian host and a vector stage. As mentioned before, leishmaniasis is transmitted by the bite of infected female sandflies, which inject promastigotes (infectious stage) during blood ingestion. Promastigotes are phagocytosed and become amastigotes, which by simple division multiply and infect mononuclear phagocytic cells. The host-parasite and various factors affect the development of different types of leishmaniasis. Sandflies become infected when they feed off a host. Within their midgut the parasites develop into promastigotes, which migrate to the salivary glands, and become infectious metacyclic promastigotes ready to infect in the new feeding. (Centers for Disease Control and Prevention, 2017) The summary of Leishmaniasis life cycle is presented in (*Figure 1*).

Leishmaniasis disease occurs in three primary forms: cutaneous, mucocutaneous, and visceral. First, cutaneous leishmaniasis (CL) is the most common form. Worldwide, annually around 600 000 to 1 million new cases are reported. CL produces skin lesions such as ulcers and

serious scars. It is known that 95% of patients who suffer from CL are localized in the Americas, the Mediterranean Basin, the Middle East, and Central Asia. (World Health Organization, 2021)

CL is present in 20 countries and it is endemic in 18 of them (Argentina, Bolivia, Brazil, Colombia, Costa Rica, Ecuador, El Salvador, Guatemala, French Guyana, Guyana, Honduras, Nicaragua, Mexico, Panama, Paraguay, Peru, Suriname and Venezuela). (Organización Panamericana de la Salud, 2021)

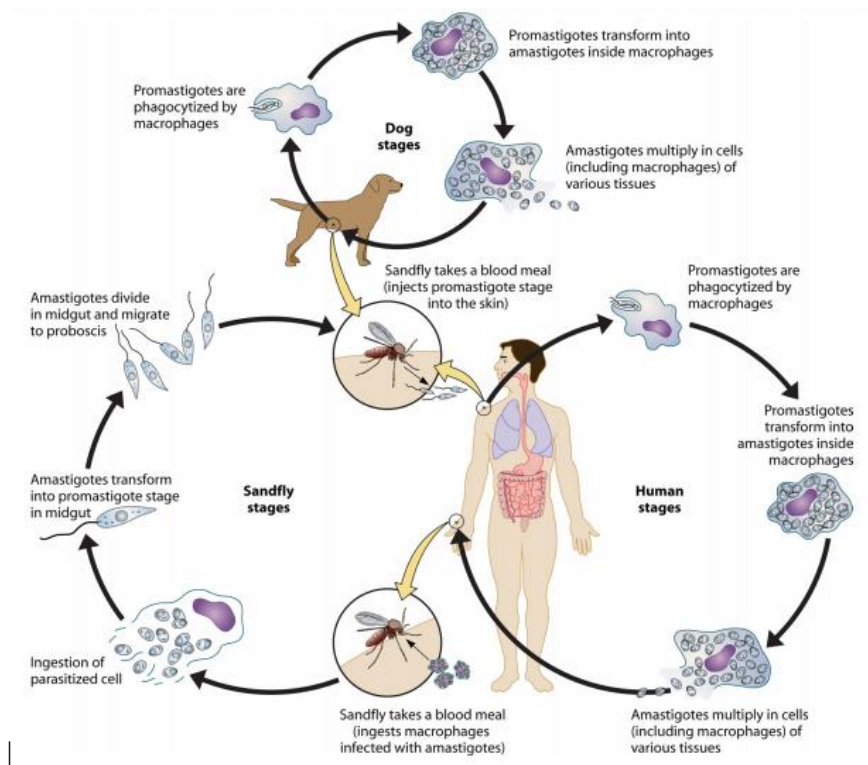


Figure 1: The life cycle of *Leishmania* species (Esch & Petersen, 2013).

Second, visceral leishmaniasis (VL) or kala-azar produces fever, weight loss, anemia, and hepatosplenomegaly (enlarged liver and spleen). If VL does not receive proper treatment, it could be mortal. Also, VL is one of the parasitic diseases capable of developing sprouts. Around the world, there are 50000 and 90000 new cases of VL; however, to World Health Organization (WHO) just has been notified between 25% and 45% of cases. Most of the cases are localized in

Brazil, China, Ethiopia, India, Iraq, Kenya, Nepal, Somalia, Sudan, and South Sudan. They represent more than 95% of cases registered by WHO. (World Health Organization, 2021)

Third, mucocutaneous leishmaniasis (ML) or "Espundia" is characterized by partial or full destruction of nose, mouth and throat mucous membranes. (World Health Organization, 2021) ML lesions spread from nasal mucosa to pharynx mucosa, larynx, and nose and lips skin. (Torres-Guerrero et al., 2017) In this way, countries like Brazil, Bolivia, Ethiopia and Peru presents 90% of ML cases. (World Health Organization, 2021) On the other hand, in the Americas, the most important species of Leishmania are *L. (L.) mexicana*, *L. (L.) amazonensis* and *L. (L.) venezuelensis* which be part of Leishmania subgenre and *L. (V.) braziliensis*, *L. (V.) panamensis*, *L. (V.) peruviana* and *L. (V.) guyanensis* which be part of Viannia subgenre. (Organización Panamericana de la Salud, 2021) The leishmania species distribution in Ecuador is showed in the next table.

In Ecuador, according to the Ministry of Public Health, the forms of leishmaniasis with the highest incidence are cutaneous and mucocutaneous. In 2018, a total of 1,268 cases were reported, of which 1,241 corresponded to CL and 27 to ML. For the year 2019, 22 of the 24 provinces of Ecuador presented cases, with a higher number of sick people in Pichincha (144), Morona Santiago (92), and Esmeraldas (86), and with a lower incidence in Guayas (4), Imbabura (4) and Carchi (1). On the other hand, leishmaniasis cases were frequent in the population between 20 and 49 years of age, with men being more prone to this disease. At the same time, children between 0 and 11 months of age reported fewer cases. (Ministry of Public Health of Ecuador, 2019) *Table 1*, adapted from (Christian & Coque, 2020) shows the leishmania species distribution by ecological region in Ecuador.

Table 1: Leishmania species distribution by ecological region in Ecuador

Species	Pacific coast	Andes	Amazon
<i>L. (V.) braziliensis</i>	x		x
<i>L.(V.) guyanensis</i>	x		x
<i>L.(V.) lainsoni</i>			x
<i>L.(V.) naiffi</i>			x
<i>L.(L.) mexicana</i>		x	
<i>L.(L.) major-like</i>		x	
<i>L.(L.) amazonensis</i>	x		



Figure 2: Cutaneous leishmaniasis on leg. (Christian & Coque, 2020)

1.2. Treatments and therapies against leishmaniasis

Nowadays, there are a variety of treatments against leishmaniasis which involve the use of drugs and therapies. (Chakravarty & Sundar, 2019) In both cases, the treatment depends on the target group (children, older adults, and pregnant or lactating women) and the type of leishmaniasis that people suffer from. (Centers for Disease Control and Prevention, 2021) In this way, the current

and emerging antileishmanial agents are miltefosine (MIL), antimonials (Sbv), and amphotericin b (AmB). MIL is an alkyl phospholipid and the unique oral drug approved for CL, VL, and ML treatment. On the other hand, the use of Sbv has been limited due to resistance development and their high toxicity causing cardiac arrhythmias, ventricular tachycardia, and others. Finally, AmB is used to treat VL by intravenous infusion.

On the other hand, the most common therapies against leishmaniasis are thermotherapy, cryotherapy, and CO₂ laser. In this way, thermotherapy is used due to Leishmania parasites do not proliferate at temperature <39°C. The treatment is cheap, no laboratory monitoring is required and minimum scarring is produced. Cryotherapy produces the cell destruction due to intracellularly ice formation, generating localized ischemic necrosis. Finally, CO₂ laser has specific thermolysis of the damaged tissue, but the healthy tissue suffers fewer effects. CO₂ laser presents side effects as hyperpigmentation, persistent redness, and hypertrophic scarring. (Chakravarty & Sundar, 2019)

1.3. Cellulose as drug delivery

Cellulose ($C_6H_{10}O_5$)_n (Figure 3) is the biopolymer most abundant on Earth. It is a linear polymer glucan that consists of tens to several thousand monosaccharides units. Also, these units are linked by $-\beta - (1 - 4) -$ glycosidic bonds. (Kögel-Knabner & Amelung, 2014; Lavanya et al., 2015) Cellulose (figure 3) is the main component of the plant walls, and it is the component of algae and fungi cell walls. (Kögel-Knabner & Amelung, 2014) In addition, cellulose presents unique biocompatibility characteristics, biodegradability, non-toxicity, good mechanical properties, and low production cost concerning other synthetic biopolymers manufacture. (Seddiqi et al., 2021)

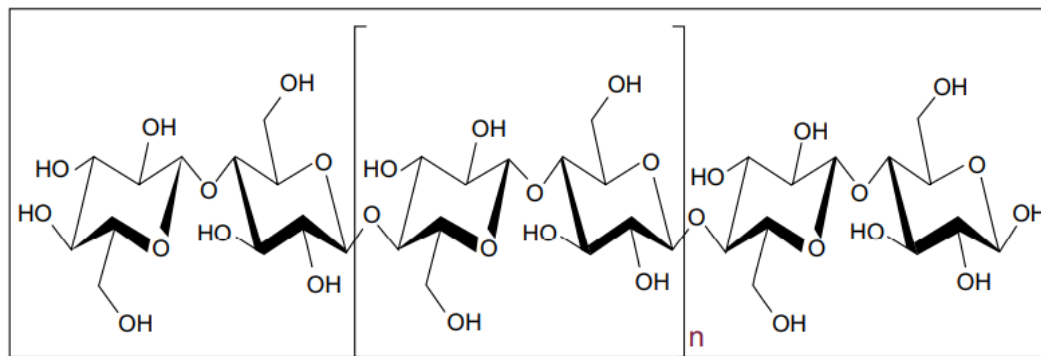


Figure 3: Chemical structure of cellulose.(George & Sabapathi, 2015)

The versatile structure of cellulose developed by modifications either by chemical or physical methods makes this biopolymer could be used for biomedical applications. (Heinze, 2015; Seddiqi et al., 2021) One of these applications is the drug delivery system, which is the drug released to different cells, tissues, or organs in appropriate time. Cellulosic materials and its derivatives promote dissolvability and excellent controllable diffusive properties. (Seddiqi et al., 2021) Finally, this polymer plays an essential role in pharmaceutical industries. (Lavanya et al., 2015)

1.4. Beads-based cellulose

Beads made from cellulose are spherical particles with diameters $\geq 10\mu\text{m}$, which are used in biomedical and biotechnological applications such as immobilization of enzymes, chromatography systems and drug delivery carriers. (Gericke et al., 2013; Voon et al., 2017) Nowadays, there is an extreme interest in cellulose beads as drug delivery systems due to their high specific surface area, high porosity, release profiles under specific conditions, and promising drug loadings. On the other hand, the internal surface area of the cellulose beads is higher (one order of magnitude) than conventional granulate materials showing that beads can loaded with huge amounts of drugs. (Gericke et al., 2013) In addition, cellulose beads have excellent thermal and mechanical

properties. (Voon et al., 2017) Also, cellulose beads are not rigid but are compressible and elastic to a certain limit. (Gericke et al., 2013)

The cellulose beads synthesis follows three main steps: dissolution of cellulose, shaping, and regeneration of the polysaccharide solution. There are different techniques reported to obtain the spherical beads; the main ones are dropping, jet cutting, and spinning drop. (Trygg et al., 2013) The dropping or dispersion technique is the formation of the spherical droplets of polysaccharide solution and its solidification on a solvent, and the size of the bead obtained varies from 0.5 to 3mm. (Gericke et al., 2013) On the other hand, nowadays, using environmentally friendly and non-derivatizing solvents to get cellulose beads is searched. For this purpose, an aqueous system is used (Trygg et al., 2013).

1.5.Methylene blue

Methylene blue ($C_{16}H_{18}ClN_3S$) is a bright blue-green dye that occurs in crystals or crystalline powder. It has a molecular weight of 319.9 and a slight odor. Methylene blue is soluble in water, ethanol, chloroform but insoluble in ethyl ether. (National Library of Medicine, 2021) This dye is within the family of phenothiazine, which is an organic compound. Methylene blue has several applications, among which its use as a dye for nucleic acids stands out due to its high binding affinity to DNA and RNA acting as a cationic dye (Encyclopaedia Britannica, 2017).

2. PROBLEM STATEMENT

2.1.Relevance to Ecuador

Currently, leishmaniasis disease is considered a public health problem for Ecuador due to the diversity of cases reported in the four natural regions of the country (the Pacific coast, the Andean slopes, the Andes, and the Amazon) (Hashiguchi et al., 2017). The predominant form of the disease is cutaneous leishmaniasis followed by mucocutaneous leishmaniasis. (Ministry of

Public Health of Ecuador, 2019) Historically, in 1920 the first case of CL was reported, in the province of Esmeraldas. Leishmaniasis occurs mainly in rural and remote areas where access to health services is relatively scarce and the lack of hospital infrastructure limits its diagnosis and correct treatment. On the other hand, the drug most used by the Ecuadorian state to treat leishmaniasis is meglumine antimoniate (Glucantime ®, Sanofi aventis), which is administered intramuscularly. However, frequently, people tend to discontinue treatment due to adverse drug reactions and long-term pain caused by injection pricks. (Hashiguchi et al., 2017)

Thus, the development of new and innovative biomaterials such as cellulose-based beads for the treatment of leishmaniasis disease represents an important advance in the way drugs are administered against this disease. People with leishmaniasis would no longer suffer the pain caused by the use of syringes because beads are for topical use which means they are in direct contact with the patient's skin and they are easy to use. In addition, due to the porosity of the beads, their load-bearing capacity is more significant, so they can hold vast amounts of medicine, sparing patients from visiting health centers regularly. Another critical point, as mentioned in previous sections is that the cost of producing cellulose-based beads is low, and the solvents with which they are made are friendly to the environment.

3. HYPOTHESIS AND OBJECTIVES

3.1.Hypothesis

Beads made from cellulose extracted from different plants can be used as a new method for drug release in the treatment of Leishmaniasis disease.

3.2.General objective

To estimate the drug release profile of beads-based cellulose loaded with fluorescent dye.

3.2.1. Specific objectives

- To extract cellulose fibers from different types of plants.
- To synthesize beads from different types of cellulose.
- To characterize the cellulose fibers using Fourier Transform Infrared Spectroscopy (FTIR).
- To characterize the cellulose beads using Scanning Electron Microscopy (SEM), Stereo Microscopy and X-Ray Nano tomography.
- To calculate the drug release profile of beads-based cellulose.
- To fit a mathematical model for drug release kinetics

4. METHODS

4.1. Materials

Table 2: Materials

Raw material	Apple, avocado, mango, and pear Commercial cellulose
Reagents	Solution A CaCl ₂ Distillated water Ethanol 99% pure Methylene blue
Material	Beakers, falcon tubes, syringe 5ml, 0.2µm filters
Equipment	Analytic balance, freezer, heating plate, lyophilizer, magnetic stir bar, sonicator, pipets, SEM, FTIR, UV-Vis spectrophotometer, vortex

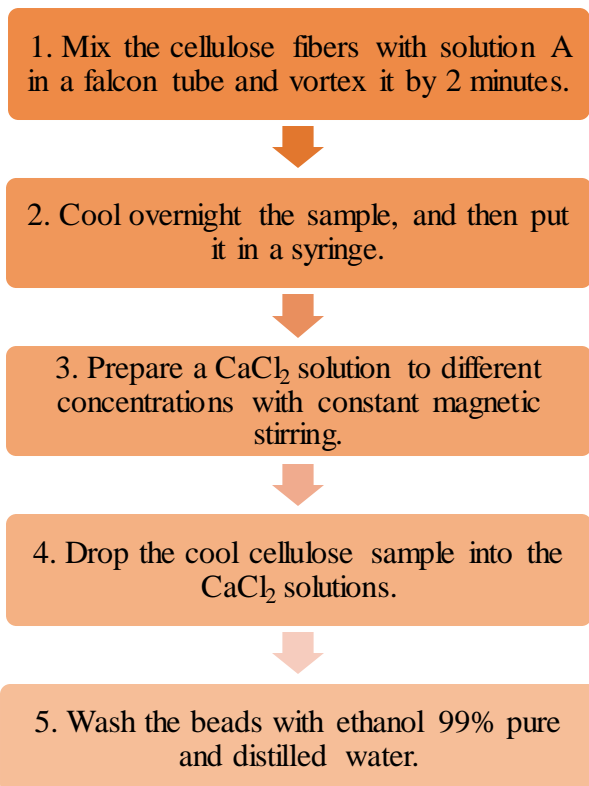
4.2. Cellulose fibers extraction

Cellulose fibers were extracted from apple, avocado, mango, and pear following different chemical processes.

4.3.Synthesis of cellulose-based beads

The cellulose-based beads were synthesized at room temperature from cellulose fibers extracted before. The synthesis process (*Scheme 1*) is similar to the one used by Serrano with some modifications. (Serrano, 2020)

Scheme 1: Process for cellulose beads synthesis



4.4.Characterization

4.4.1. Cellulose fibers characterization

Fourier-transform infrared spectroscopy (FTIR) spectra of apple, avocado, mango, and pear cellulose were recorded in the range of $\sim 4000\text{-}40\text{ cm}^{-1}$ using a Cary 630 FTIR Spectrometer to determine the functional groups of the cellulose fibers and to verify if there is no presence of molecules as hemicellulose or lignin. An XRD Diffractometer Rigaku Miniflex for X-Ray Diffraction (XRD) analysis was used to determine the crystalline nature of each fiber cellulose sample.

4.4.2. Beads characterization

Phenom ProX Scanning Electron Microscope (SEM) was used to determine the morphology and porosity of the cellulose beads from apple and mango. In addition, the size of the beads was determined using a stereomicroscope Olympus LS to different magnifications. Finally, an X-Ray Nano tomography was used to analyze the internal structure of cellulose beads.

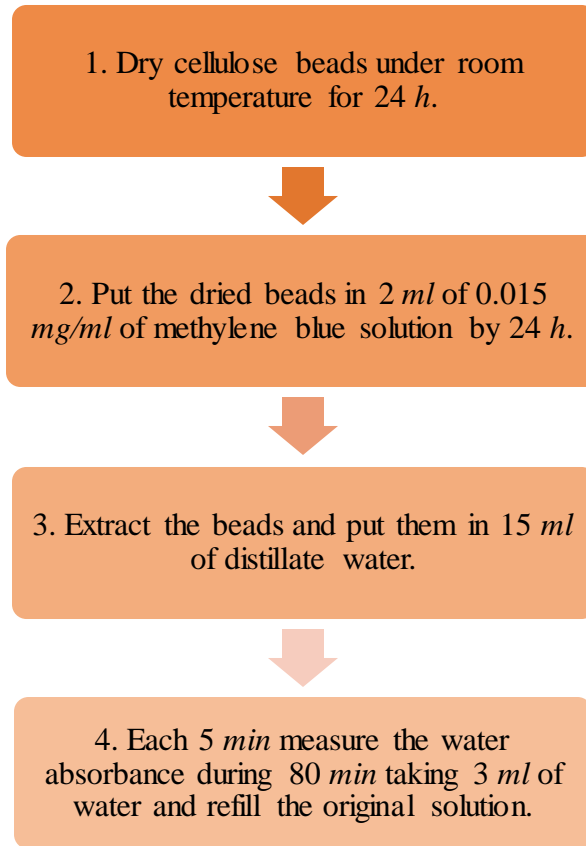
4.4.3. Drug profile release

In this work, the drug release profile was analyzed using the methylene blue dye as a replacement for common medications (model drug) used for the treatment of leishmaniasis.

The calibration curve of the dye was determined from 100 ml of a 0.1 *mg/ml* methylene blue solution. The dilutions made were 0.10, 0.25, 0.50, 0.75, 1, 3, 5, 7, 9, 11 $\mu\text{g/ml}$. The samples were measured using a spectrophotometer and using distilled water as a blank. In addition, the spectral sweep of methylene blue was carried out to find the appropriate wavelength for the analysis of the samples.

For the encapsulation of the dye in the cellulose beads, some modifications were made to the protocol carried out by Zeng and collaborators. (Zeng et al., 2020) *Scheme 2* shows the encapsulation process and absorbance measurement.

Scheme 2: Encapsulation of methylene blue in the cellulose beads



4.5. Release Kinetics Analysis

The release kinetics from apple, mango, and commercial cellulose beads were analyzed using different mathematical models: zero-order, first-order, Higuchi, Korsmeyer-Peppas, and Hixson-Crowell.

5. RESULTS, INTERPRETATION, AND DISSCUSION

5.1. Cellulose fibers extraction

Cellulose fibers from apple, mango, avocado, and pear were extracted (*Figure 4*). As a result, the fibers are white in color and have a soft texture. In the case of avocado cellulose (*Figure 4C*), the fibers are oily.

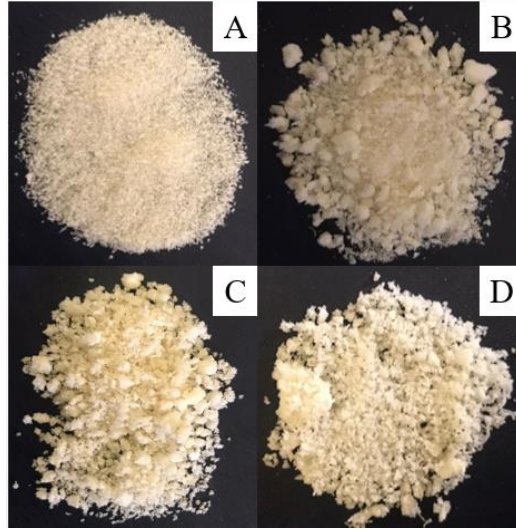


Figure 4: Cellulose fibers from (A) apple, (B) mango, (C) avocado, and (D) pear

5.2. Cellulose fibers characterization

5.2.1. Fourier-transform infrared spectroscopy

Before the X-Ray study, the cellulose samples were pulverized. The FTIR spectra of the cellulose fibers from apple (Figure 5), mango (Figure 6), avocado (Figure 7), pear (Figure 8), and commercial (Figure 9) were compared with the FTIR spectrum of commercial cellulose determined by Aqil and collaborators. (Aqil et al., 2015) In this way, the identification of absorption bands for all samples was as follows: the hydroxyl group OH stretching vibration peaks are between $\sim 3200\text{ cm}^{-1}$ and $\sim 3270\text{ cm}^{-1}$. The C-H stretching vibration peaks are between $\sim 2801\text{ cm}^{-1}$ and $\sim 2922\text{ cm}^{-1}$. The OH bending of absorbed water peak varies between $\sim 1594\text{ cm}^{-1}$ and $\sim 1632\text{ cm}^{-1}$. The CH₂ rocking vibrations peaks range from $\sim 1409\text{ cm}^{-1}$ to $\sim 1422\text{ cm}^{-1}$. Finally, the C-O-C glycosidic ether band peaks vary between $\sim 894\text{ cm}^{-1}$ and $\sim 953\text{ cm}^{-1}$. Table 3 presents a summary with the complete values for each cellulose and absorption band peak.

Table 3: Absorption band peaks from cellulose fibers

GROUPS	ABSORPTION BAND PEAKS (cm^{-1})				
	Apple	Mango	Avocado	Pear	Commercial
Hydroxyl group OH stretching vibration	3265.50	3260.01	3337.62	3287.42	3201.78
C-H stretching vibration	2885.49	2889.68	2922.09	2883.87	2801.09
OH bending of absorbed water	1598.29	1594.31	1600.16	1602.66	1632.57
CH ₂ rocking vibrations	1409.64	1407.36	1419.23	1419.72	1422.67
C-O-C glycosidic ether band	895.49	953.87	897.29	895.13	894.56

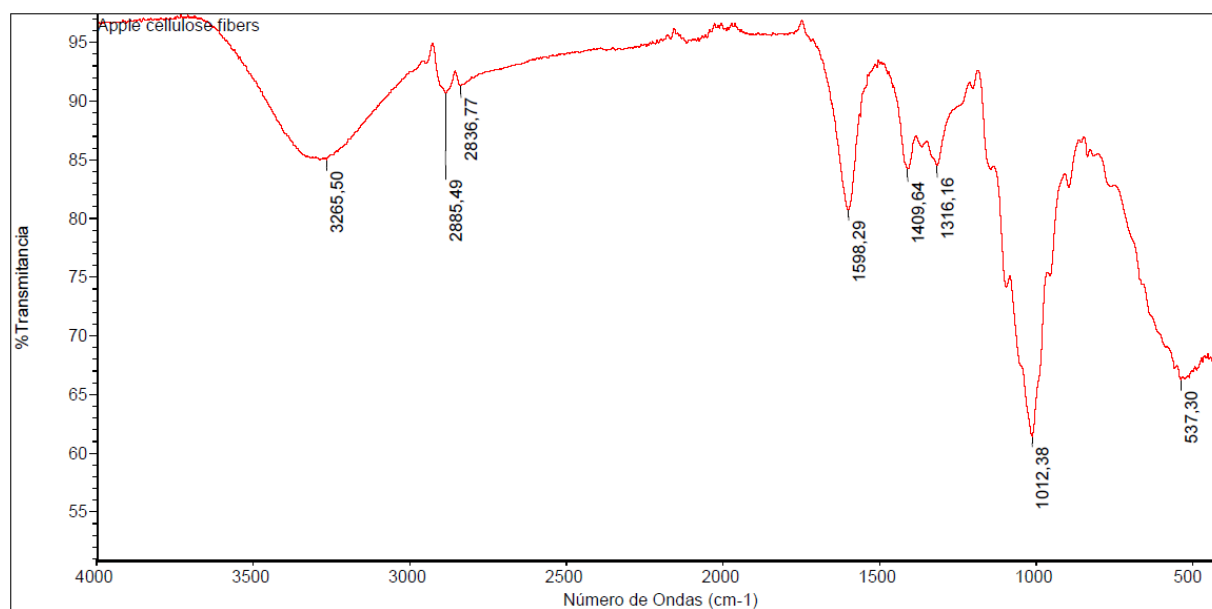


Figure 5: FTIR analysis of apple cellulose fibers

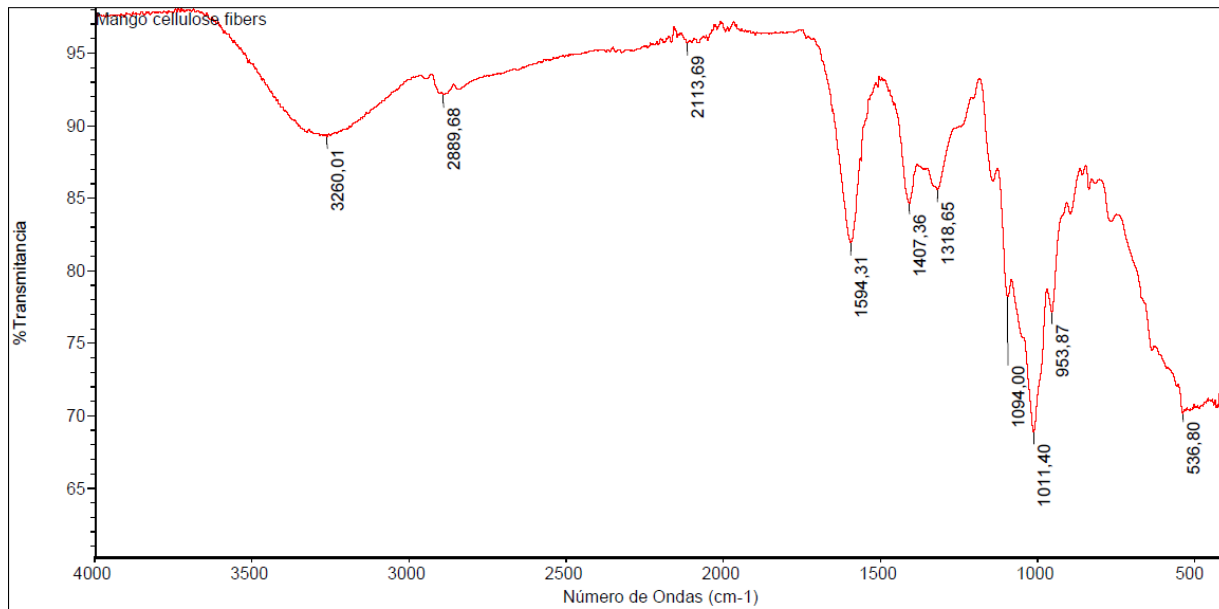


Figure 6: FTIR analysis of mango cellulose fibers

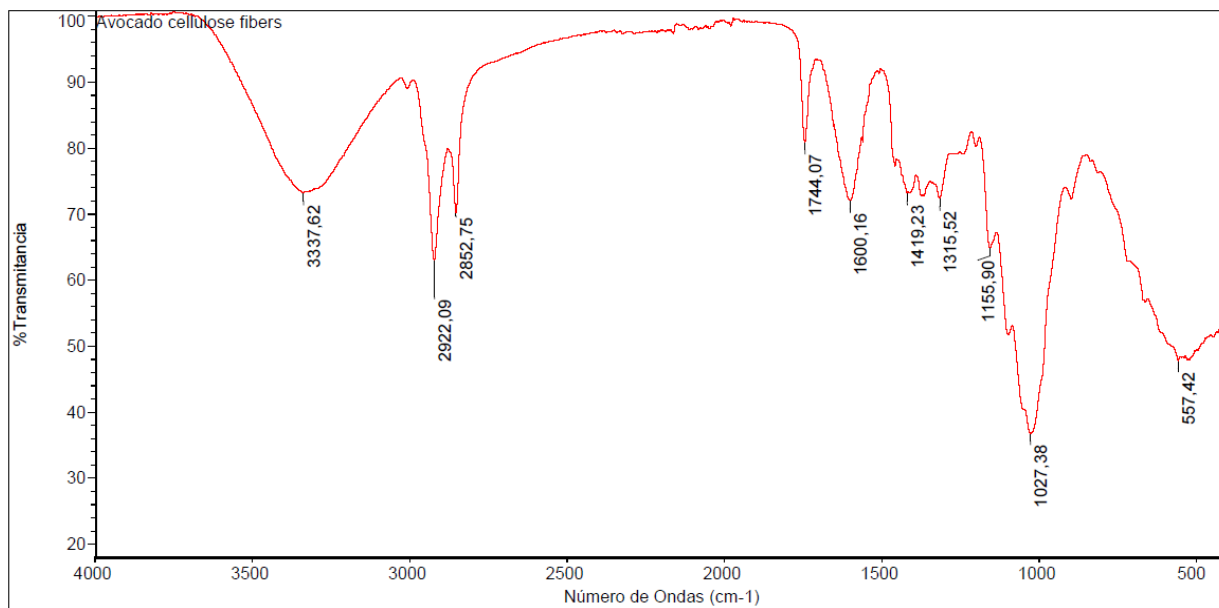


Figure 7: FTIR analysis of avocado cellulose fibers

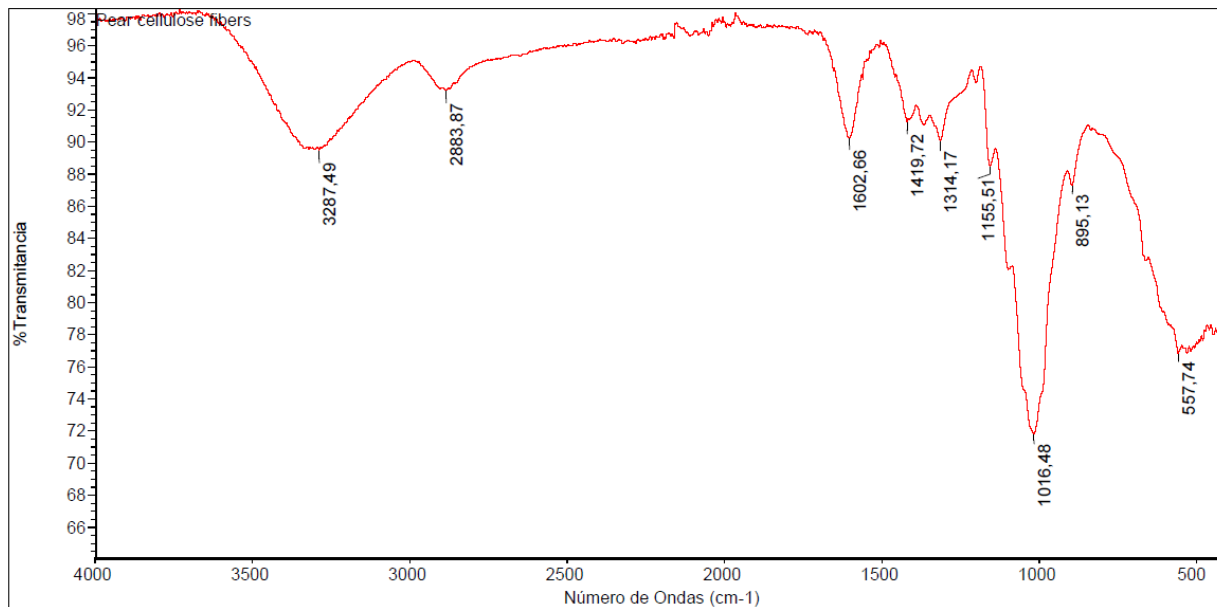


Figure 8: FTIR analysis of pear cellulose fibers

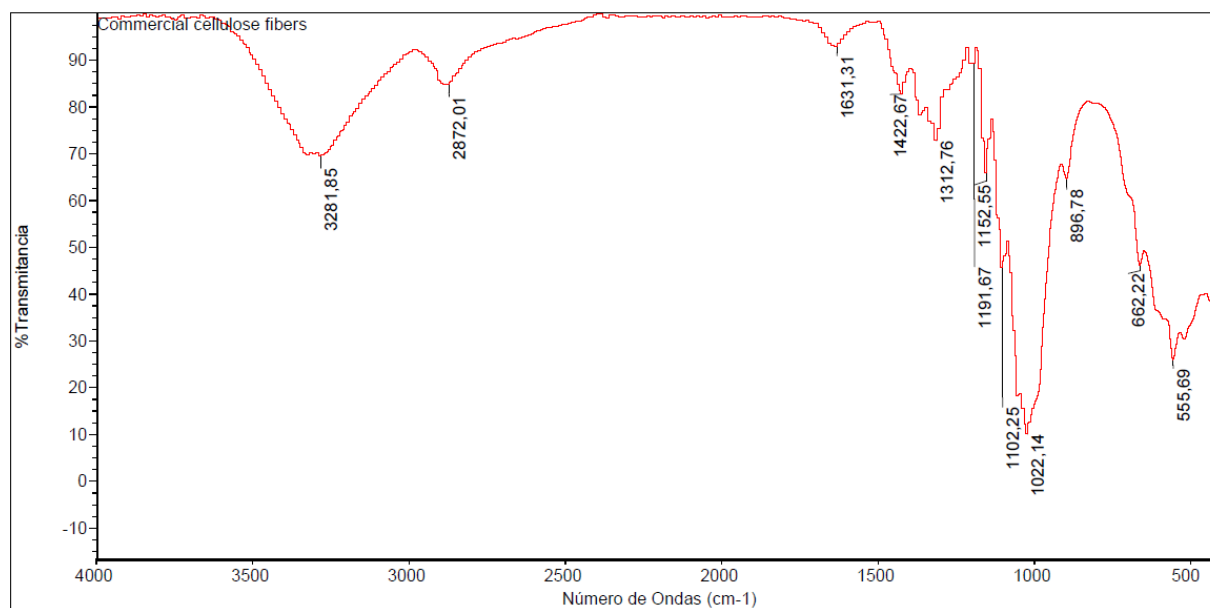


Figure 9: FTIR analysis of commercial cellulose fibers

5.2.2. X-Ray Diffraction

To calculate the cellulose crystallinity index (Table 4), the XRD peak high method was used. (Segal et al., 1959) Commercial cellulose (Figure 14) has the highest crystallinity index among the studied fibers with 81.33%, followed by mango fibers (Figure 11) with 53.96%, apple

(Figure 10) with 53.96%, and pear (Figure 13) with 36.08%. Finally, the cellulose with the lowest crystallinity index was avocado (Figure 12) with 1.05%.

$$CrI = \frac{(I_{002} - I_{am})}{I_{002}} \times 100$$

Equation 1: Crystallinity Index

Table 4: Cellulose crystallinity Index

Cellulose fibers	Cellulose Crystallinity Index			
	I_{002}	I_{am}	CrI	CrI(%)
Apple	16383,86	7542,74	0,54	53,96
Mango	6638,12	2310,96	0,65	65,19
Avocado	22592,09	22355,38	0,01	1,05
Pear	18069,10	11550,59	0,36	36,08
Commercial	89872,98	16597,60	0,82	81,53

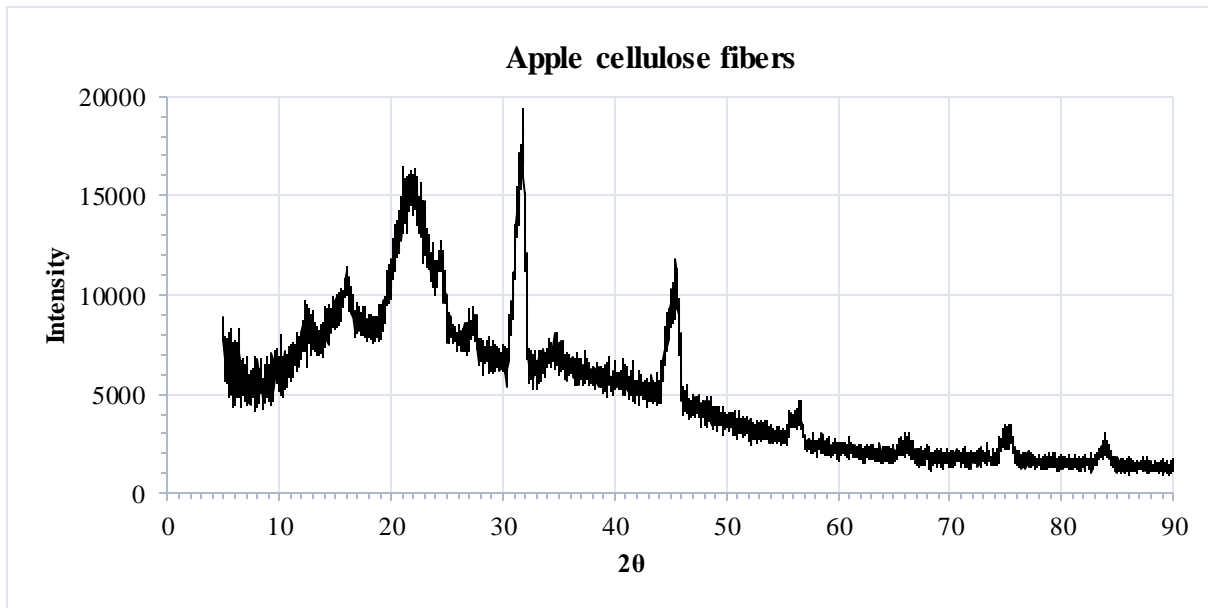


Figure 10: X-Ray Diffraction of the apple cellulose fibers

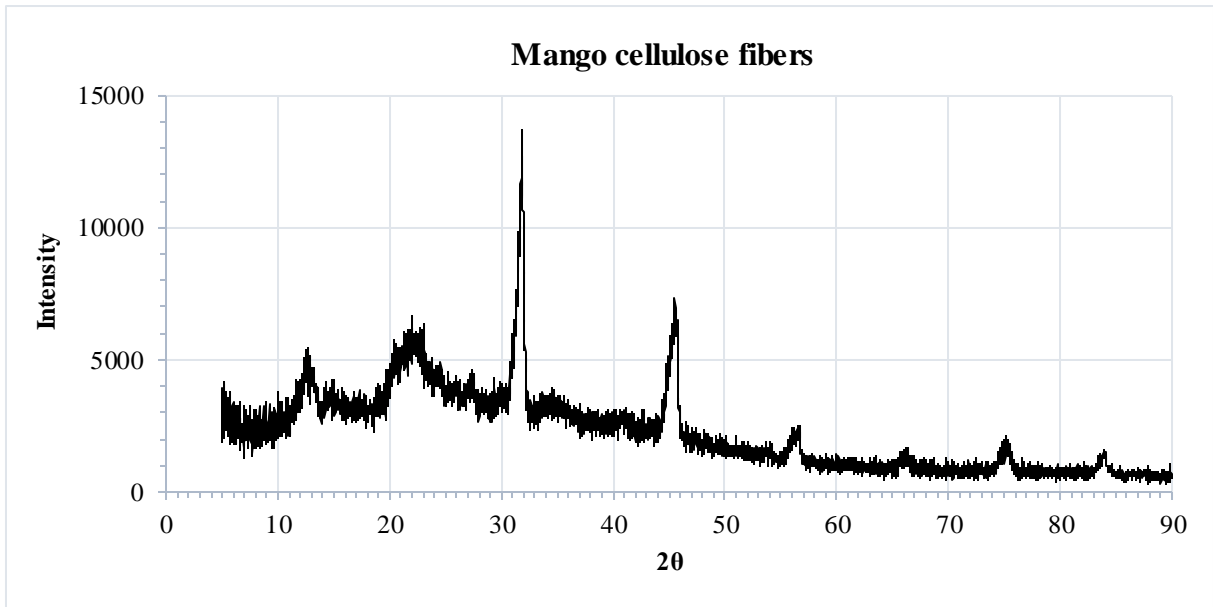


Figure 11: X-Ray Diffraction of the mango cellulose fibers

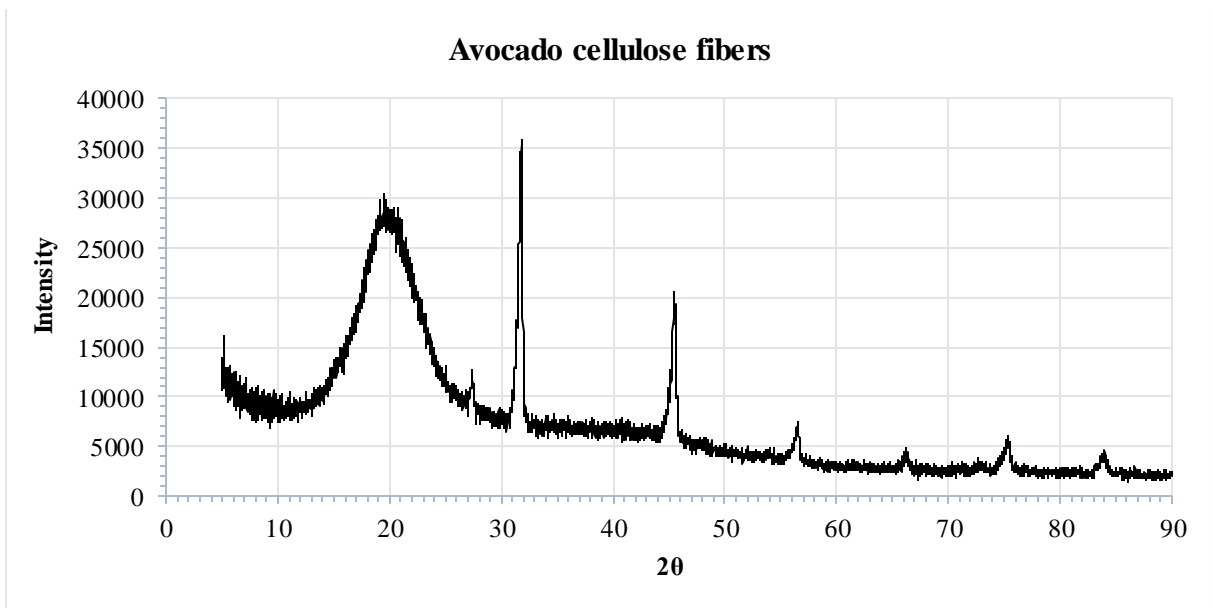


Figure 12: X-Ray Diffraction of the avocado cellulose fibers

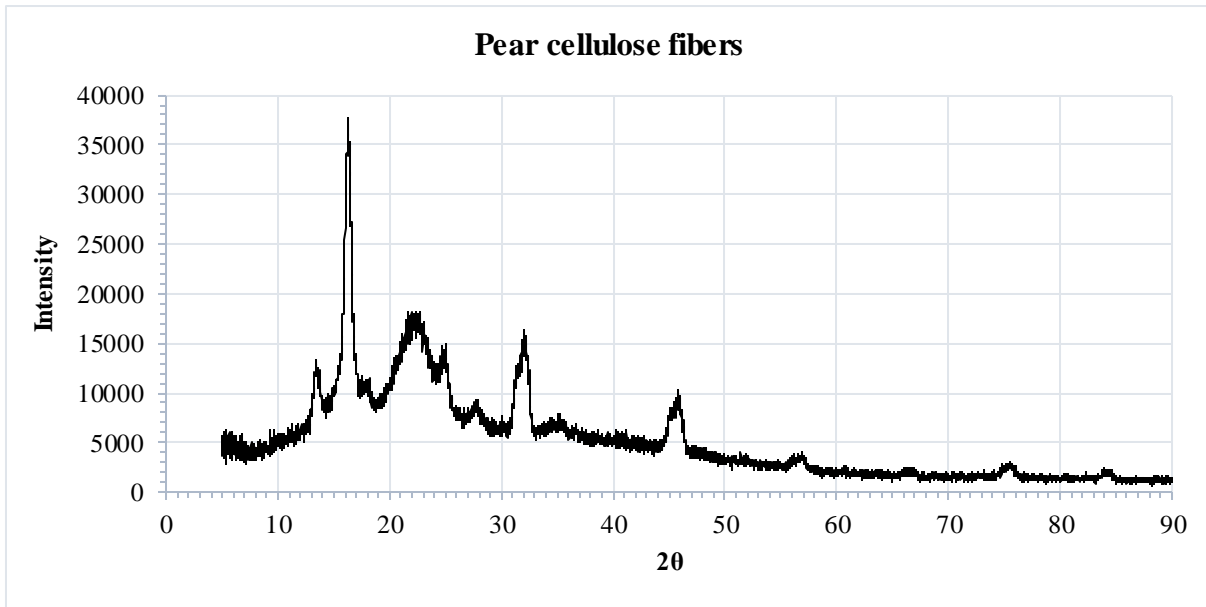


Figure 13: X-Ray Diffraction of the pear cellulose fibers

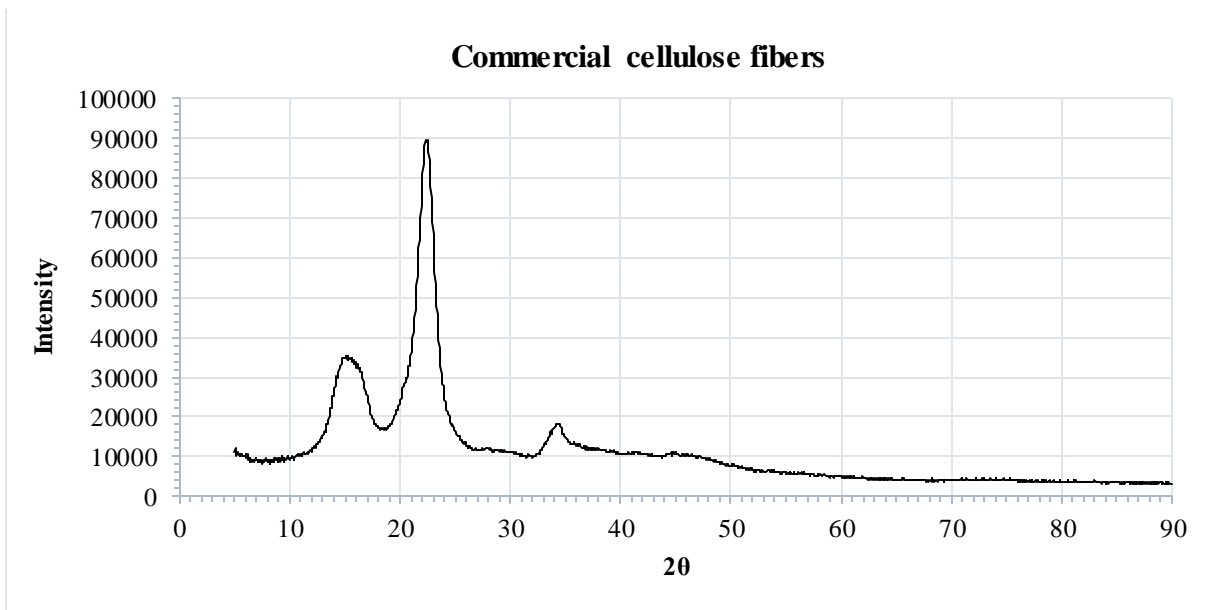


Figure 14: X-Ray Diffraction of the commercial cellulose fibers

5.3. Cellulose beads synthesis

The synthesis of beads was carried out at different concentrations of CaCl_2 to determine what would be the optimal concentration at which the cellulose beads would acquire their spherical shape. The bead formation process was studied for 4 different types of cellulose, which come from apple, mango, avocado, and pear. In addition, commercial cellulose was added to the analysis. The

pH for all cellulose solutions was basic. In this way, the apple solution pH was 14.65, the mango solution 14.40, and the commercial solution was 14.07. The values were estimated using a pH meter and were corroborated using pH test strips.

In this way, it turned out that cellulose from apple (*Figure 15*) and mango (*Figure 16*) coagulate, and as a result formed beads at 1 M and 1.2 M concentrations, while commercial cellulose (*Figure 17*) formed beads at 0.8 M, 1 M, and 1.2 M. As a result, beads of regular spherical shape and hard consistency were obtained. However, avocado (*Figure 18*) and pear (*Figure 19*) fibers cellulose did not form beads. In both cases, cellulose solutions do not coagulate properly. *Table 1* summarizes the formation of beads in CaCl₂ solutions.

Finally, as shown in images (*Figures 15-17*), at higher the CaCl₂ concentration, the greater the formation of cellulose beads. These results agree with what was stated by Nie and collaborators mentioning that the higher the concentration of calcium ions, the greater the number of synergistic interactions in the chains of cellulose that dissolve, and then, the harder cellulose beads will be. (Nie et al., 2021)

Table 5: Results of cellulose beads synthesis from different cellulose fibers

Cellulose fibers	Bead synthesis at different CaCl ₂ concentrations					
	0.2 M	0.4 M	0.6 M	0.8 M	1.0 M	1.2 M
Apple	No	No	No	No	Yes	Yes
Avocado	No	No	No	No	No	No
Mango	No	No	No	No	Yes	Yes
Pear	No	No	No	No	No	No
Commercial	No	No	No	Yes	Yes	Yes

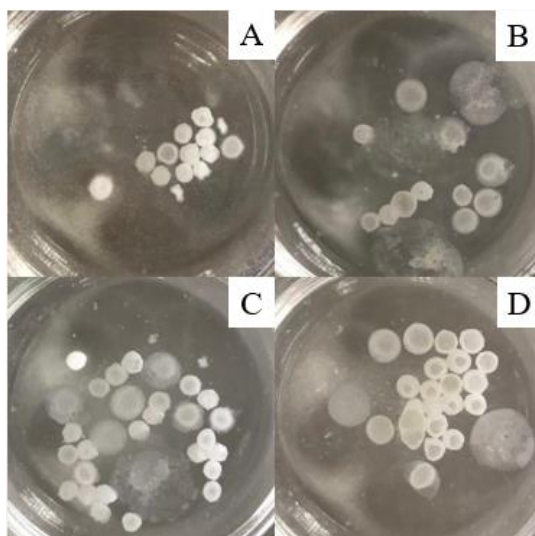


Figure 15: Cellulose beads synthesized from apple at different CaCl_2 concentrations (A)0.6 M, (B)0.8 M, (C)1 M, and (D)1.2 M

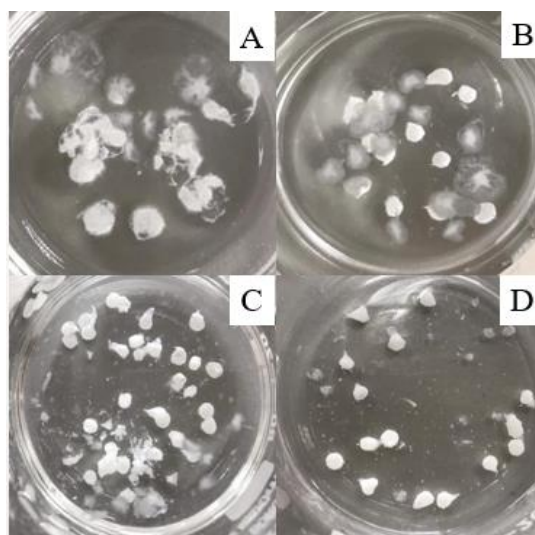


Figure 16: Cellulose beads synthesized from mango at different CaCl_2 concentrations (A)0.6 M, (B)0.8 M, (C)1 M, and (D)1.2 M

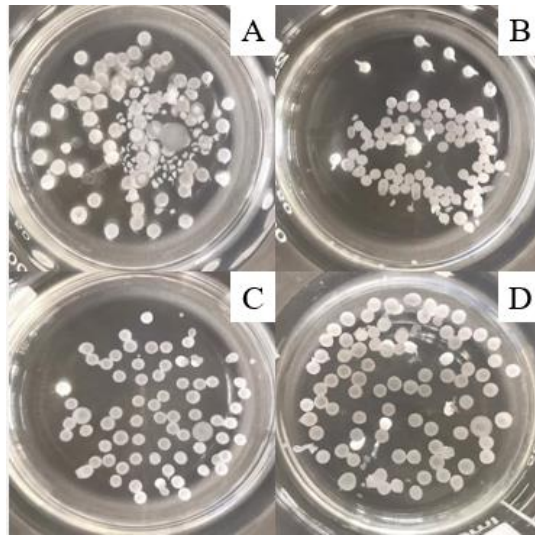


Figure 17: Cellulose beads synthesized from commercial cellulose at different CaCl_2 concentrations (A) 0.6 M, (B) 0.8 M, (C) 1 M, and (D) 1.2 M

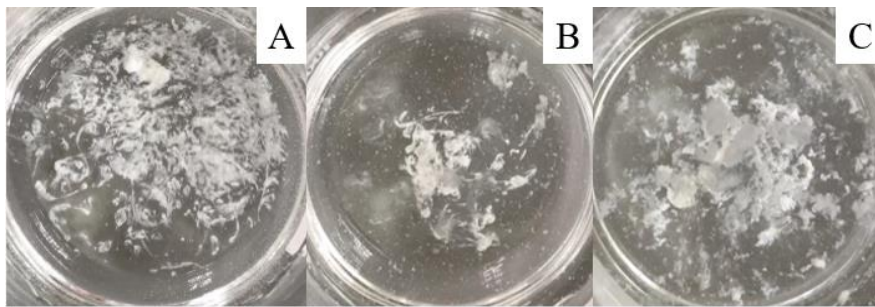


Figure 18: Cellulose beads synthesized from avocado cellulose at different CaCl_2 concentrations (A) 0.6 M, (B) 0.8 M, and (C) 1 M

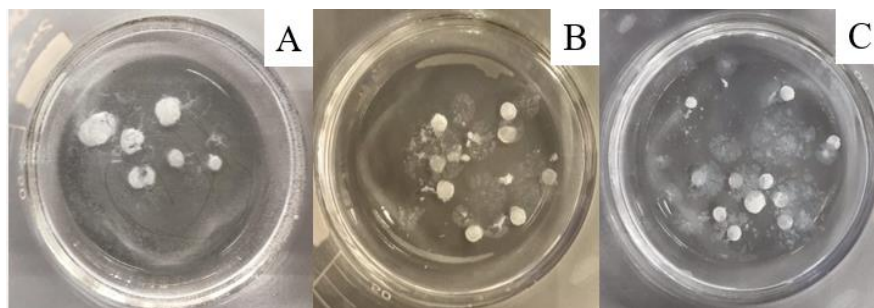


Figure 19: Cellulose beads synthesized from pear cellulose at different CaCl_2 concentrations (A) 0.6 M, (B) 0.8 M, and (C) 1 M

5.4. Cellulose beads characterization

5.4.1. Stereo Microscope

To determinate the cellulose size beads, beads from apple, mango, and commercial cellulose were prepared previously at 1 M CaCl₂, with the CaCl₂ pH at 7.86. The samples were dried and then analyzed under a stereomicroscope at 3.2x magnification.

The size of each cellulose bead was determined by taking two different length measures for each bead; as a result, the mean length was obtained. The smallest beads were from mango cellulose (*Figure 25*), the average size was 1.41 cm. Followed by apple beads (*Figure 24*) whose size was 1.44 cm, and the biggest ones were from commercial cellulose (*Figure 26*) with 1.52 cm. The results are shown in *Table 6*, and complete data is presented in *Annex A*.

Table 6: Size of cellulose beads

Cellulose beads	Size	
	Mean (cm)	S.D.
Apple	1.44	0.21
Mango	1.41	0.09
Commercial	1.52	0.16

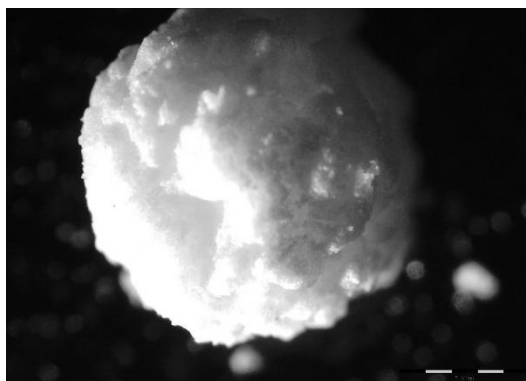


Figure 20: Dried apple cellulose bead prepared at 1 M CaCl₂ solution under a stereo microscope at 3.2x

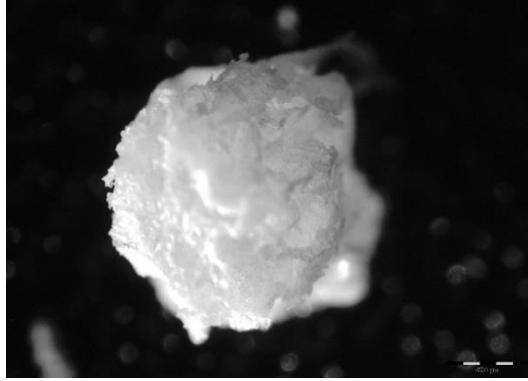


Figure 21: Dried mango cellulose bead prepared at 1 M CaCl₂ solution under a stereo microscope at 3.2x

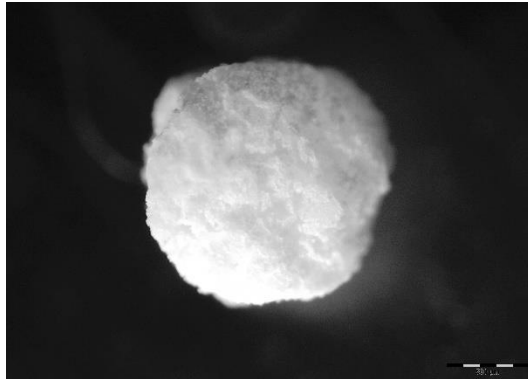


Figure 22: Dried commercial cellulose bead prepared at 1 M CaCl₂ solution under a stereo microscope at 3.2x

5.4.2. Scanning Electron Microscopy

The bead samples were prepared in a 1 M CaCl₂ solution and then dried. The outer crust of apple cellulose beads (*Figure 20*) shows pores of length $\sim 3\mu\text{m}$ and small globules of $\sim 5\mu\text{m}$ forming a network to each other. As for the mango cellulose beads (*Figure 21*) present pores length of $\sim 5\mu\text{m}$ and globules of $\sim 4\mu\text{m}$, and fragmentation of the rind can be seen. Finally, the commercial cellulose beads (*Figure 22*) have pores of length $\sim 9\mu\text{m}$ and globules of $\sim 19\mu\text{m}$. In this way, due to the fact the pore size of commercial cellulose beads being larger than those of apple and mango beads, their loading capacity could be more significant than the other analyzed beads since there is a correlation between loading capacity and pore size. (Zeng et al., 2020)

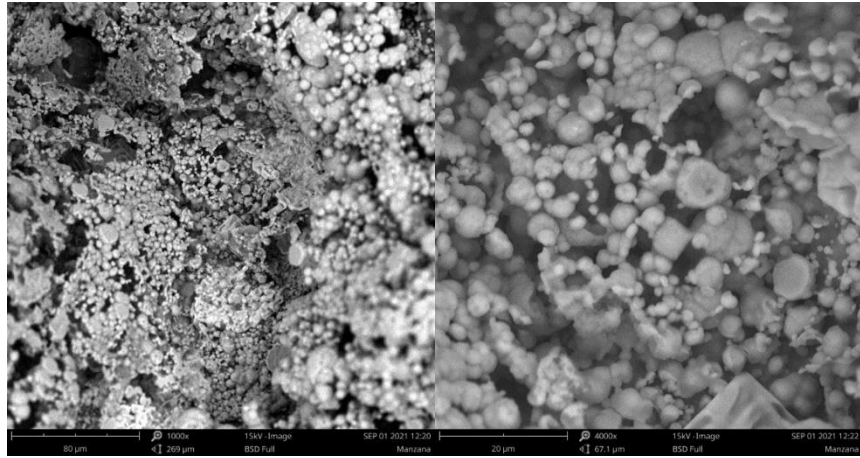


Figure 23: SEM analysis from apple cellulose beads

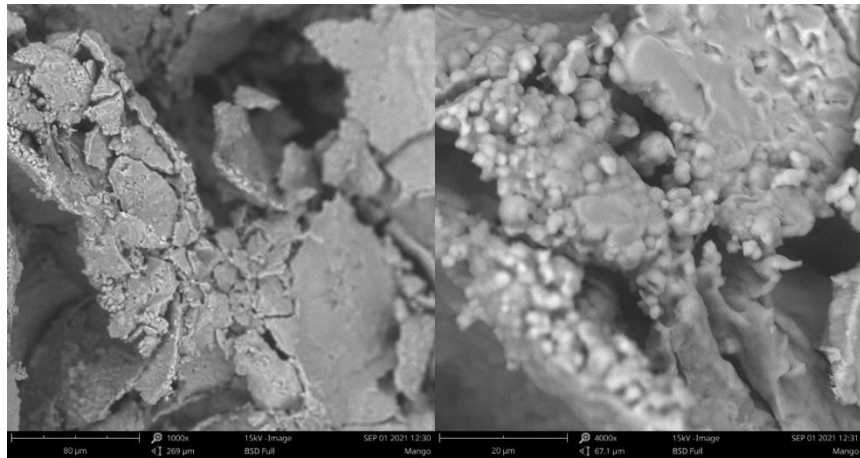


Figure 24: SEM analysis from mango cellulose beads.

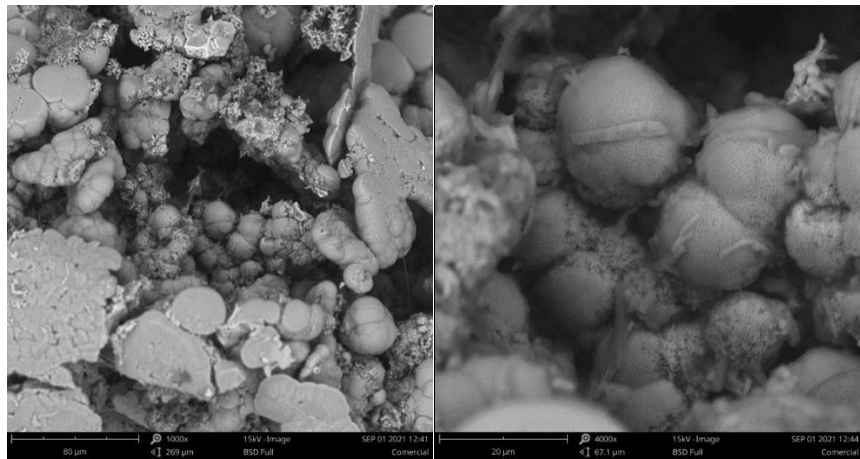


Figure 25: SEM analysis from commercial cellulose beads.

5.4.3. X-Ray Nano tomography Analysis

An X-Ray Nano tomography analyzed the internal structure from apple and commercial cellulose beads. *Figure 26A* shows an apple bead sample with an internal network of pores and globules of small size, as shown in *Figure 23*. In addition, the commercial cellulose (*Figure 26B*), shows bigger pores and globules as analyzed before in *Figure 25*. Thus, the external and internal structures of the beads have similar characteristics.

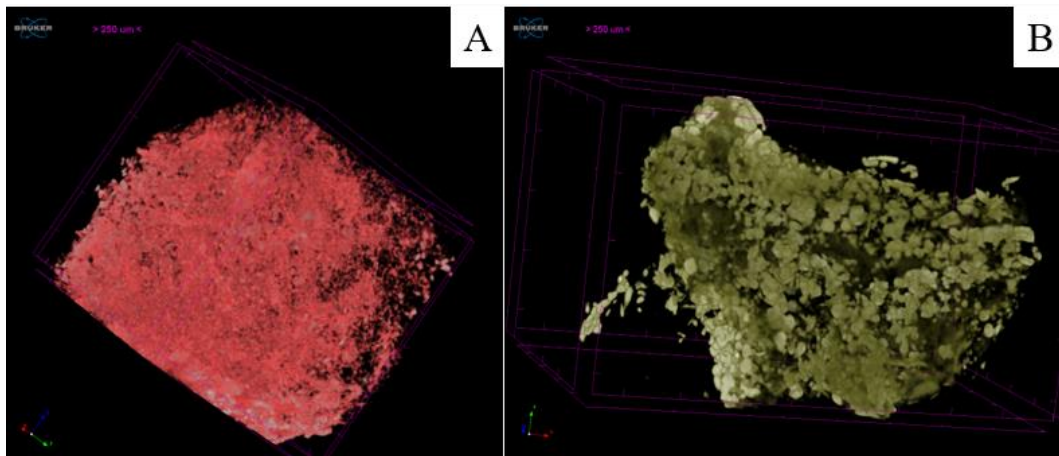


Figure 26: X-Ray Nanotomography analysis from cellulose beads. (A) apple bead, and (B) commercial bead

5.5. Release profile

The spectral sweep of the methylene blue stock solution (*Annex B*) to find the maximum wavelength (λ_{max}) was 663.42 nm. With this λ_{max} , the methylene blue calibration curve (*Figure 27*) was estimated and it was obtained that the concentration [$\mu\text{g/ml}$] is the absorbance value divided by 202.79, also, the R^2 value of the curve was 0.998. The data to get the calibration curve is presented in *Annex C*.

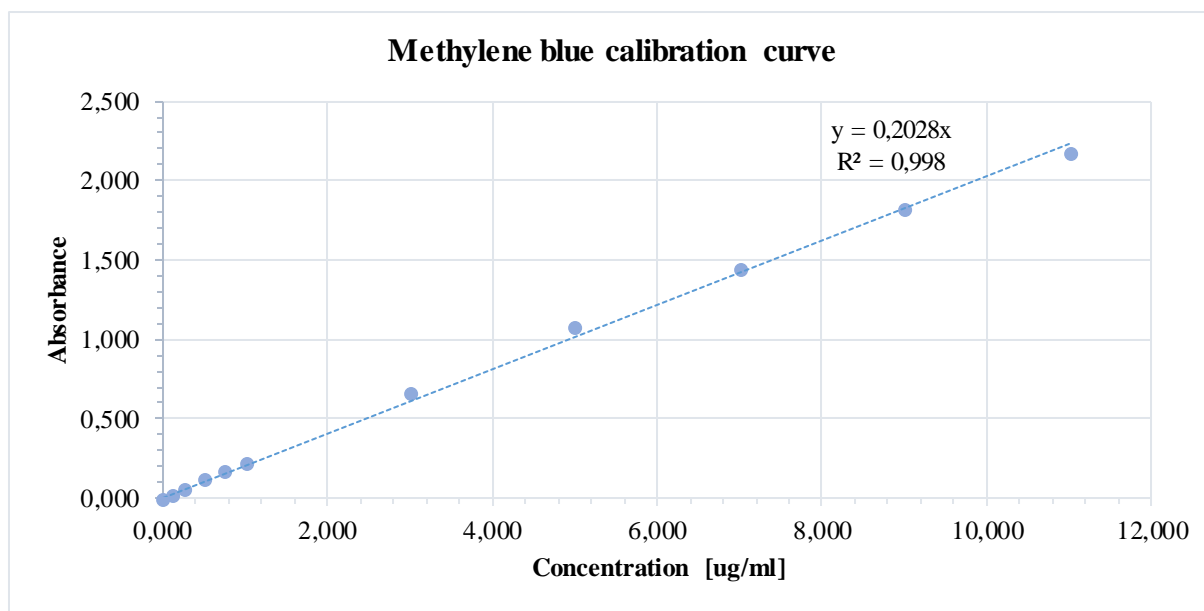


Figure 27: Methylene blue calibration curve

To drug release profile study, 25 beads of apple, mango, and commercial cellulose were chosen and loaded with 2 ml of 0.015 mg/ml methylene blue. The beads were then placed in 15 ml of distilled water (Figure 28). During 80 min in 5 min intervals, its absorbance was measured at a wavelength of 663.42 nm, which was previously estimated. The process was repeated three times for each type of cellulose. Once the absorbance was obtained, the concentration of methylene blue in the distilled water was determined for each period, and the percentage of the dye released by the beads was also calculated.

The methylene blue release behavior shows a controlled release, in Figure 29 it is observed that mango and commercial cellulose beads have the same release profile until minute 15, but from minute 20 their behavior changes, as a result, mango beads release the dye faster than commercial cellulose beads. On the other hand, apple beads release methylene blue in less time than the previously mentioned beads.

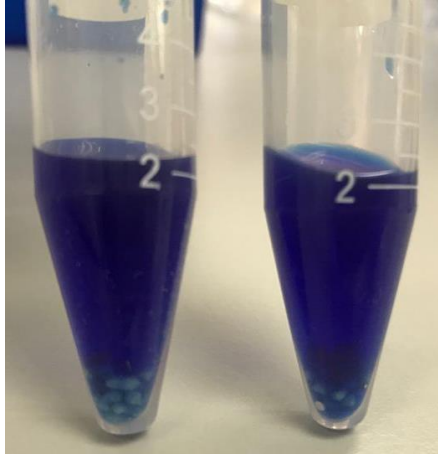


Figure 28: Methylene blue solution and cellulose beads

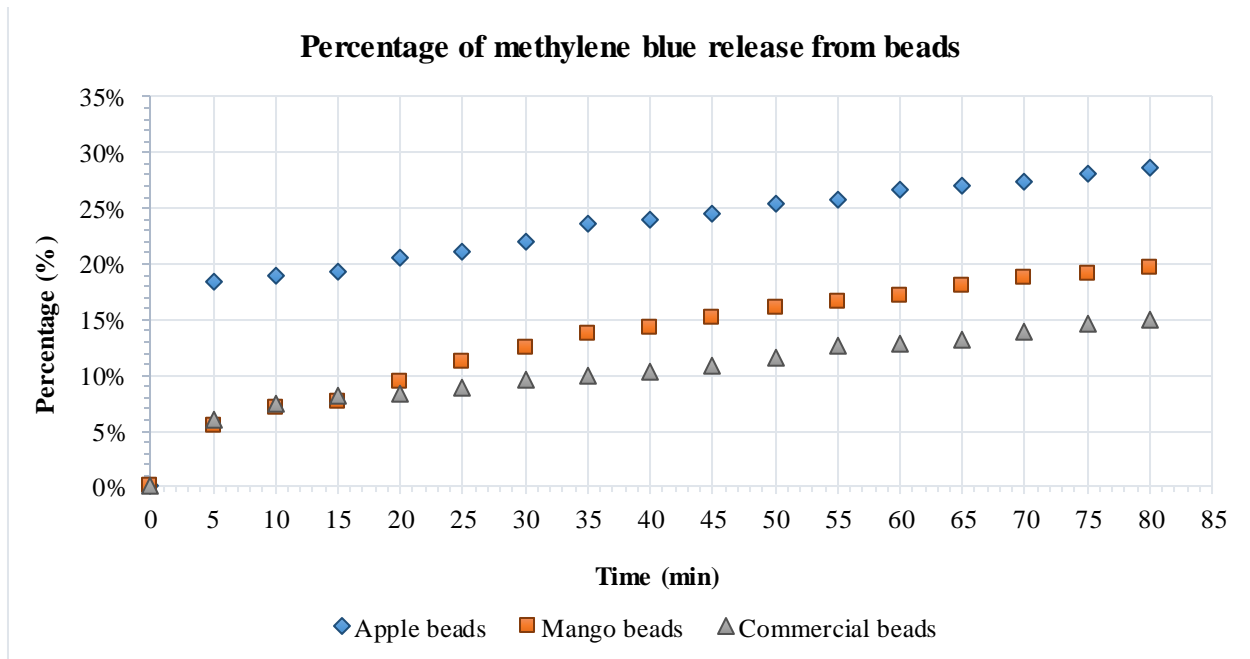


Figure 29: Percentage of methylene blue release from beads vs. time

Finally, it was observed that in 80 min the apple beads released 28.6% of methylene blue, the mango beads released 19.56%, and the commercial cellulose beads released 14.96%. The absorbance and percent release results are shown in *Table 7*, and the complete data is in *Annex D*.

Table 7: Results of methylene blue release from cellulose beads

Time (min)	ABSORBANCE VALUES						PERCENTAGE OF METHYLENE BLUE RELEASE FROM BEADS %					
	Apple beads		Mango beads		Commercial beads		Apple beads		Mango beads		Commercial beads	
	Mean	S.D.	Mean	S.D.	Mean	S.D.	Mean	S.D.	Mean	S.D.	Mean	S.D.
0	0,000	0,000	0,000	0,000	0,000	0,000	0,00%	0,00%	0,00%	0,00%	0,00%	0,00%
5	0,075	0,002	0,022	0,002	0,025	0,001	18,41%	0,51%	5,51%	0,51%	6,08%	0,28%
10	0,077	0,004	0,028	0,004	0,030	0,002	18,98%	0,99%	6,99%	0,93%	7,48%	0,38%
15	0,078	0,004	0,031	0,005	0,033	0,003	19,31%	1,03%	7,64%	1,28%	8,14%	0,65%
20	0,083	0,005	0,038	0,006	0,033	0,003	20,46%	1,13%	9,45%	1,36%	8,38%	0,65%
25	0,085	0,004	0,045	0,003	0,036	0,002	21,04%	1,03%	11,18%	0,79%	8,79%	0,51%
30	0,089	0,003	0,045	0,002	0,039	0,001	21,94%	0,85%	12,41%	1,11%	9,62%	0,25%
35	0,095	0,005	0,055	0,003	0,038	0,001	23,50%	1,14%	13,64%	0,75%	9,86%	0,49%
40	0,097	0,006	0,056	0,002	0,042	0,003	23,92%	1,50%	14,30%	0,49%	10,27%	0,62%
45	0,099	0,006	0,060	0,001	0,041	0,003	24,49%	1,36%	15,12%	0,38%	10,93%	0,38%
50	0,103	0,007	0,065	0,001	0,043	0,002	25,39%	1,78%	16,03%	0,25%	11,51%	0,51%
55	0,105	0,007	0,066	0,001	0,051	0,003	25,81%	1,75%	16,52%	0,25%	12,57%	0,65%
60	0,108	0,008	0,070	0,001	0,052	0,002	26,63%	1,96%	17,18%	0,14%	12,74%	0,51%
65	0,110	0,008	0,073	0,002	0,054	0,003	27,04%	1,99%	18,00%	0,43%	13,23%	0,62%
70	0,111	0,009	0,068	0,001	0,057	0,003	27,37%	2,11%	18,82%	0,79%	13,97%	0,75%
75	0,114	0,008	0,078	0,003	0,057	0,003	28,11%	1,86%	19,15%	0,71%	14,55%	0,25%
80	0,116	0,010	0,079	0,007	0,058	0,003	28,60%	2,47%	19,56%	1,75%	14,96%	0,14%

5.6. Kinetics Release Model

The release kinetics of methylene blue from different cellulose beads was evaluated through five types of mathematical models commonly used for the study of drug release kinetics: zero-order model, first-order model, Higuchi model, Korsmeyer-Peppas model, and Hixson-Crowell model. (Baishya, 2017)

In this way, based on the coefficient of determination R^2 and the value of the Akaike Information Criterion (AIC), it was determined that for the three types of cellulose beads, the model that best fits is the First Order kinetic model due to there is a correlation between R^2 and AIC. Thus, for apple beads $R^2 = 0.6826$ and $AIC = -2.9163$, for mango beads $R^2 = 0.9355$ and $AIC = -3.1231$, and for commercial cellulose beads $R^2 = 0.8736$ and $AIC = -3.5084$. In other words, the

release rate is proportional to the methylene blue that remains within the cellulose beads. Figure 30 shows the first-order model.

The data from the first-order model was determined for the three beads types, following *Equation 2*.

Equation 2: First order kinetic equation

$$\log C = \log C_0 - \frac{K_1 t}{2.303}$$

Where K_1 is the first-order rate equation, C_0 is the initial concentration of the drug, and C is the percent of drug remaining at time t . To this study, the equation from linear regression is $y = -0,0011x - 0,066$ for apple beads, $y = -0,001x - 0,0198$ for mango beads and $-0,0007x - 0,021$ for commercial beads.

On the other hand, the Higuchi kinetic model could also be considered, due to higher R^2 values, however, the AIC values are lower than First Order kinetic equation AIC values. *Table 8* shows the data obtained for cellulose beads. Complete kinetic model plots are shown in *Figures 31-34*.

In the literature, there are no studies that evaluate the release kinetics using methylene blue dye loading in apple, mango, and commercial cellulose beads. Studies made with other types of compounds loading in beads have been identified such as using bovine serum albumin (BSA). (Nie et al., 2021)

Table 8: The r^2 , adjusted R^2 and AIC values from different mathematical models used to analyze the methylene blue kinetics release from apple, mango, and commercial cellulose beads

Kinetic Model	r^2			Adjusted R^2			AIC		
	Apple beads	Mango beads	Commercial beads	Apple beads	Mango beads	Commercial beads	Apple beads	Mango beads	Commercial beads
Zero order	0.6472	0.9236	0.8638	0,6237	0,9186	0,8547	0,6101	0,4519	0,0937
First order	0.7024	0.9395	0.8815	0,6826	0,9355	0,8736	-2,9163	-3,1231	-3,5084
Higuchi	0.8428	0.9957	0.9652	0,8323	0,9954	0,9629	-2,3441	-2,5024	-2,8605
Hixson-Crowell	0.6472	0.8638	0.9636	0,6237	0,9186	0,8547	-3,1981	-3,3878	-3,7640
Korsmeyer-Peppas	0.2018	0.0357	0.1638	0,1486	-0,0285	0,1081	-1,5623	-1,1245	-1,1602

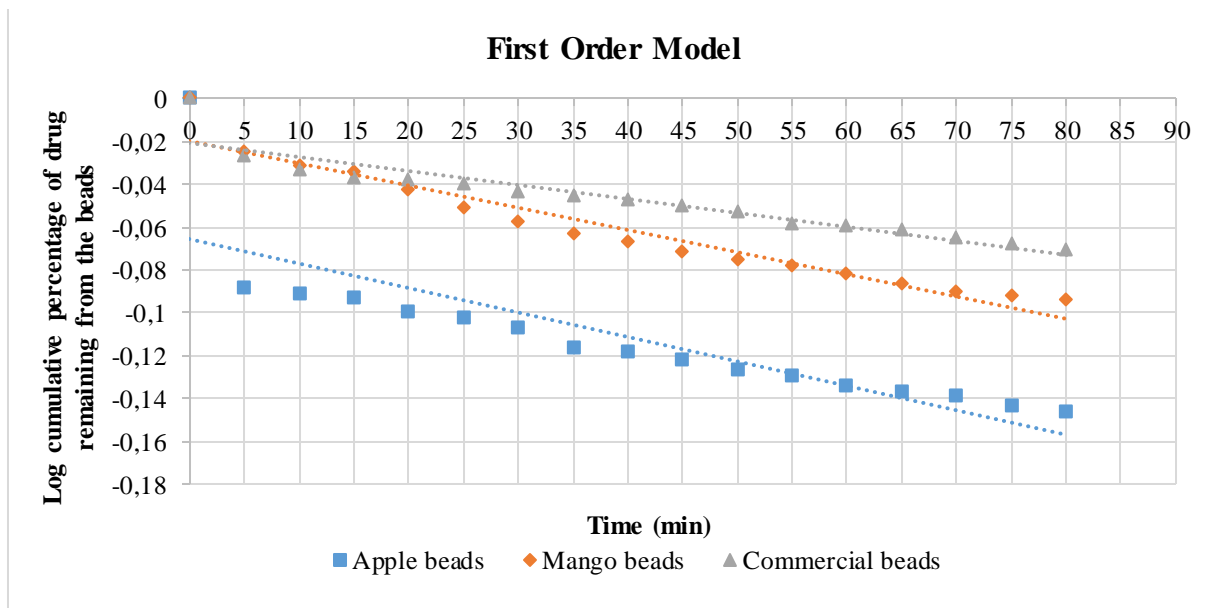


Figure 30: First Order drug release model from apple, mango and commercial cellulose

6. CONCLUSIONS AND RECOMMENDATIONS

Cellulose fibers from apple, mango, avocado, and pear were successfully synthesized by different processes. Thus, FTIR observed the presence of functional groups characteristic of cellulose was observed, determining the absence of lignin or hemicellulose in the samples. Additionally, using X-Ray Diffraction, the crystallinity index of the fibers was calculated. Commercial cellulose has 81.53%, mango cellulose 65.19%, apple cellulose 53.96%, pear cellulose 36.08%, and avocado cellulose 1.05%.

On the other hand, cellulose-based beads were successfully synthesized at 0.8 M, 1 M, and 1.2 M CaCl_2 using apple, mango, and commercial cellulose fibers. Thus, the synthesized beads were white, hard in consistency, and alkaline pH because their primary compounds were also alkaline. Regarding size, the largest beads were commercial cellulose (1.52cm), and the smallest were those of mango cellulose (1.41cm). Additionally, the pore size presented by each type of bead was analyzed, with commercial cellulose being larger ($\sim 9\mu\text{m}$), and apple cellulose smaller ($\sim 3\mu\text{m}$).

In this study, the release profile of cellulose-based beads was also analyzed using methylene blue dye. Beads were loaded with 0.015mg/ml of dye and placed in 15ml of distilled water for 80 min; as a result, it was obtained that the apple beads released $\sim 29\%$ of the loaded dye, the mango beads $\sim 20\%$, and beads of commercial cellulose $\sim 15\%$, being the fastest release with apple beads.

Additionally, it was estimated that the kinetic model that best fits cellulose-based beads is first-order kinetics, generating a correlation between R^2 and AIC. That is, the release rate is proportional to the amount of methylene blue that remains in the beads. Thus, for apple cellulose

beads $R^2 = 0.6826$ and $AIC = -2.9163$, for mango beads $R^2 = 0.9355$ and $AIC = -3.1231$, and for commercial cellulose beads $R^2 = 0.8736$ and $AIC = -3.5084$.

Finally, commercial apple, mango, and cellulose beads could potentially be used as a new and innovative method for the encapsulation and release of drugs used in the treatment against leishmaniasis due to the small size of the beads, which would allow their easy application. Also due to their porosity, large amounts of drugs could be loaded into them. This new method of drug delivery makes it possible to avoid the use of intrusive procedures such as the application of drugs through syringes, improving the quality of life of patients.

Future works

It is essential to load the cellulose-based beads with drugs used against leishmaniasis and to study their behavior.

In vitro assays using *Leishmania*, cell cultures are essential.

Synthesized beads-based cellulose using cellulose from different endemic plants.

7. REFERENCES

- Aqil, M., Abderrahim, B., Abderrahman, E., Mohamed, A., Fatima, T., Abdesselam, T., & Krim, O. (2015). Kinetic Thermal Degradation of Cellulose, Polybutylene Succinate and a Green Composite: Comparative Study. *World Journal of Environmental Engineering*, 3(4), 95–110. <https://doi.org/10.12691/wjee-3-4-1>
- Baishya, H. (2017). Application of Mathematical Models in Drug Release Kinetics of Carbidopa and Levodopa ER Tablets. *Journal of Developing Drugs*, 06(02), 1–8. <https://doi.org/10.4172/2329-6631.1000171>
- Centers for Disease Control and Prevention. (2017). *Leishmaniasis*. <https://www.cdc.gov/dpdx/leishmaniasis/index.html>
- Centers for Disease Control and Prevention. (2021). *CDC - Leishmaniasis - Resources for Health Professionals*.
- Chakravarty, J., & Sundar, S. (2019). *Current and emerging medications for the treatment of leishmaniasis*. <https://sci-hub.se/10.1080/14656566.2019.1609940>
- Christian, M. T., & Coque. (2020). *Leishmaniasis in Ecuador: A bibliographic review*. 4(1), 21–27. <https://medicienciasuta.uta.edu.ec/index.php/MedicienciasUTA>
- Encyclopaedia Britannica. (2017). *Methylene blue*. <https://www.britannica.com/science/methylene-blue>
- Esch, K. J., & Petersen, C. A. (2013). *Transmission and Epidemiology of Zoonotic Protozoal Diseases of Companion Animals*. <https://doi.org/10.1128/CMR.00067-12>
- George, J., & Sabapathi, S. N. (2015). Cellulose nanocrystals: Synthesis, functional properties, and applications. *Nanotechnology, Science and Applications*, 8, 45–54. <https://doi.org/10.2147/NSA.S64386>
- Gericke, M., Trygg, J., & Fardim, P. (2013). Functional cellulose beads: Preparation, characterization, and applications. *Chemical Reviews*, 113(7), 4812–4836. <https://doi.org/10.1021/cr300242j>
- Hashiguchi, Y., Velez, L. N., Villegas, N. V., Mimori, T., Gomez, E. A. L., & Kato, H. (2017). Leishmaniasis in Ecuador: Comprehensive review and current status. *Acta Tropica*, 166, 299–315. <https://doi.org/10.1016/j.actatropica.2016.11.039>
- Heinze, T. (2015). Cellulose: Structure and properties. *Advances in Polymer Science*, 271, 1–52. https://doi.org/10.1007/12_2015_319

- Kögel-Knabner, I., & Amelung, W. (2014). Dynamics, Chemistry, and Preservation of Organic Matter in Soils. *Treatise on Geochemistry: Second Edition*, 12, 157–215.
<https://doi.org/10.1016/B978-0-08-095975-7.01012-3>
- Lavanya, D., Kulkarni, P. K., Dixit, M., Prudhvi Kanth Raavi, & L.Naga Vamsi Krishna. (2015). Sources of cellulose and their applications- A review INTERNATIONAL JOURNAL OF DRUG FORMULATION AND RESEARCH SOURCES OF CELLULOSE AND THEIR APPLICATIONS –. *International Journal of Drug Formulation and Research*, 2(January 2011), 19–38.
- Ministry of Public Health of Ecuador. (2019). *SUBSISTEMA DE VIGILANCIA SIVE-ALERTA ENFERMEDADES TRANSMITIDAS POR VECTORES ECUADOR, SE 1-32 / 2019*.
<https://www.who.int/es/news-room/fact-sheets/detail/dengue-and-severe-dengue>
- National Library of Medicine. (2021). *Methylene blue Compound Summary*.
<https://pubchem.ncbi.nlm.nih.gov/compound/Methylene-blue>
- Nie, G., Zang, Y., Yue, W., Wang, M., Baride, A., Sigdel, A., & Janaswamy, S. (2021). Cellulose-based hydrogel beads: Preparation and characterization. *Carbohydrate Polymer Technologies and Applications*, 2, 100074. <https://doi.org/10.1016/J.CARPTA.2021.100074>
- Organización Panamericana de la Salud. (2021). *Leishmaniasis cutánea y mucosa*.
<https://www.paho.org/es/temas/leishmaniasis/leishmaniasis-cutanea-mucosa>
- Seddiqi, H., Oliaei, E., Honarkar, H., Jin, J., Geonzon, L. C., Bacabac, R. G., & Klein-Nulend, J. (2021). Cellulose and its derivatives: towards biomedical applications. *Cellulose*, 28(4), 1893–1931. <https://doi.org/10.1007/s10570-020-03674-w>
- Segal, L., Creely, J. J., Martin, A. E., & Conrad, C. M. (1959). An Empirical Method for Estimating the Degree of Crystallinity of Native Cellulose Using the X-Ray Diffractometer. *Textile Research Journal*, 29(10), 786–794. <https://doi.org/10.1177/004051755902901003>
- Serrano, C. (2020). *UNIVERSIDAD DE INVESTIGACIÓN DE TECNOLOGÍA Escuela de Ciencias Biológicas e Ingeniería*.
- Torres-Guerrero, E., Quintanilla-Cedillo, M. R., Ruiz-Esmenjaud, J., & Arenas, R. (2017). Leishmaniasis: a review. *F1000Research*, 6.
<https://doi.org/10.12688/F1000RESEARCH.11120.1>
- Trygg, J., Fardim, P., Gericke, M., Mäkilä, E., & Salonen, J. (2013). Physicochemical design of the morphology and ultrastructure of cellulose beads. *Carbohydrate Polymers*, 93(1), 291–

299. <https://doi.org/10.1016/j.carbpol.2012.03.085>

Voon, L. K., Pang, S. C., & Chin, S. F. (2017). Porous Cellulose Beads Fabricated from Regenerated Cellulose as Potential Drug Delivery Carriers. *Journal of Chemistry*, 2017. <https://doi.org/10.1155/2017/1943432>

World Health Organization. (2021). *Leishmaniasis*. <https://www.who.int/es/news-room/fact-sheets/detail/leishmaniasis>

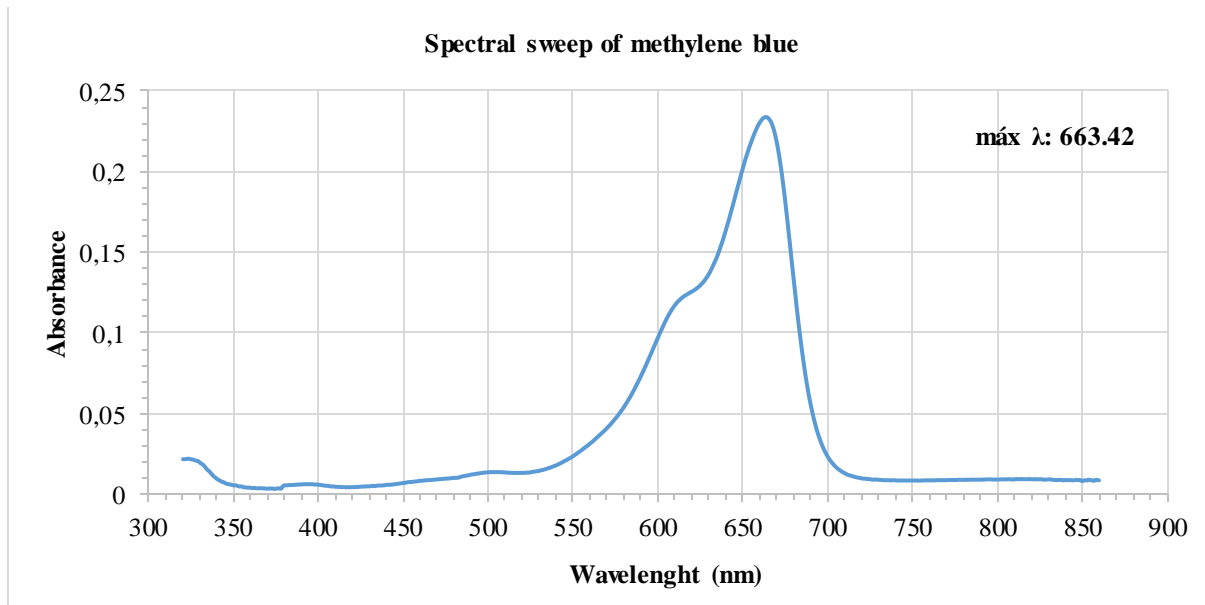
Zeng, B., Wang, X., & Byrne, N. (2020). Cellulose beads derived from waste textiles for drug delivery. *Polymers*, 12(7). <https://doi.org/10.3390/polym12071621>

8. ANNEXES

Annex A: Complete table with the data obtained from beads size

Apple beads		Mango beads		Commercial beads	
Length 1 (cm)	Length 2 (cm)	Length 1 (cm)	Length 2 (cm)	Length 1 (cm)	Length 2 (cm)
1,96	1,95	1,36	1,77	1,41	1,48
1,44	1,50	1,41	1,43	1,50	1,59
1,47	1,46	1,45	1,43	1,53	1,69
1,34	1,29	1,33	1,34	1,50	1,66
1,29	1,35	1,36	1,34	1,77	1,76
1,43	1,35	1,42	1,43	1,59	1,41
1,48	1,46	1,36	1,31	1,10	1,41
1,43	1,42	1,45	1,42	1,34	1,52
1,56	1,33	1,42	1,43	1,45	1,43
1,07	1,18	1,40	1,40	1,70	1,68
Mean	1,44	Mean	1,41	Mean	1,52
S.D.	0,21	S.D.	0,09	S.D.	0,16

Annex B: Spectral sweep of the methylene blue stock solution



Annex C: Complete table with data to obtain the methylene blue calibration

Concentration [ug/ml]	Absorbance
0.00	0.0000
0.10	0.0217
0.25	0.0589
0.50	0.1175
0.75	0.1719
1.00	0.2237
3.00	0.6689
5.00	1.0723
7.00	1.4400
9.00	1.8265
11.00	2.1694

ANNEX D: Complete data of absorbance, concentration, amount of drug release from beads, and percentage of drug release from beads from apple, mango and commercial cellulose

Time (min)	ABSORBANCE														
	APPLE BEADS					MANGO BEADS					COMMERCIAL BEADS				
	Sample 1	Sample 2	Sample 3	Mean	S.D.	Sample 1	Sample 2	Sample 3	Mean	S.D.	Sample 1	Sample 2	Sample 3	Mean	S.D.
0	0,000	0,000	0,000	0,000	0,000	0,000	0,000	0,000	0,000	0,000	0,000	0,000	0,000	0,000	0,000
5	0,077	0,074	0,073	0,075	0,002	0,020	0,023	0,024	0,022	0,002	0,026	0,024	0,024	0,025	0,001
10	0,081	0,077	0,073	0,077	0,004	0,024	0,030	0,031	0,028	0,004	0,032	0,029	0,030	0,030	0,002
15	0,083	0,077	0,075	0,078	0,004	0,025	0,034	0,034	0,031	0,005	0,036	0,032	0,031	0,033	0,003
20	0,088	0,082	0,079	0,083	0,005	0,032	0,042	0,041	0,038	0,006	0,037	0,033	0,032	0,034	0,003
25	0,090	0,084	0,082	0,085	0,004	0,043	0,044	0,049	0,045	0,003	0,038	0,034	0,035	0,036	0,002
30	0,093	0,087	0,087	0,089	0,003	0,046	0,055	0,050	0,050	0,005	0,040	0,038	0,039	0,039	0,001
35	0,098	0,098	0,090	0,095	0,005	0,052	0,058	0,056	0,055	0,003	0,042	0,038	0,040	0,040	0,002
40	0,100	0,101	0,090	0,097	0,006	0,056	0,060	0,058	0,058	0,002	0,044	0,039	0,042	0,042	0,003
45	0,102	0,103	0,093	0,099	0,006	0,060	0,063	0,061	0,061	0,002	0,046	0,043	0,044	0,044	0,002
50	0,105	0,109	0,095	0,103	0,007	0,064	0,066	0,065	0,065	0,001	0,049	0,045	0,046	0,047	0,002
55	0,106	0,111	0,097	0,105	0,007	0,066	0,068	0,067	0,067	0,001	0,054	0,050	0,049	0,051	0,003
60	0,111	0,114	0,099	0,108	0,008	0,070	0,069	0,070	0,070	0,001	0,054	0,050	0,051	0,052	0,002
65	0,111	0,117	0,101	0,110	0,008	0,074	0,071	0,074	0,073	0,002	0,056	0,051	0,054	0,054	0,003
70	0,112	0,119	0,102	0,111	0,009	0,080	0,074	0,075	0,076	0,003	0,060	0,054	0,056	0,057	0,003
75	0,115	0,121	0,106	0,114	0,008	0,081	0,076	0,076	0,078	0,003	0,060	0,058	0,059	0,059	0,001
80	0,116	0,126	0,106	0,116	0,010	0,078	0,073	0,087	0,079	0,007	0,061	0,060	0,061	0,061	0,001

CONCENTRATION [$\mu\text{g/ml}$]														
APPLE BEADS					MANGO BEADS					COMMERCIAL BEADS				
Sample 1	Sample 2	Sample 3	Mean	S.D.	Sample 1	Sample 2	Sample 3	Mean	S.D.	Sample 1	Sample 2	Sample 3	Mean	S.D.
0,000	0,000	0,000	0,000	0,000	0,000	0,000	0,000	0,000	0,000	0,000	0,000	0,000	0,000	0,000
0,380	0,365	0,360	0,368	0,010	0,099	0,113	0,118	0,110	0,010	0,128	0,118	0,118	0,122	0,006
0,399	0,380	0,360	0,380	0,020	0,118	0,148	0,153	0,140	0,019	0,158	0,143	0,148	0,150	0,008
0,409	0,380	0,370	0,386	0,021	0,123	0,168	0,168	0,153	0,026	0,178	0,158	0,153	0,163	0,013
0,434	0,404	0,390	0,409	0,023	0,158	0,207	0,202	0,189	0,027	0,182	0,163	0,158	0,168	0,013
0,444	0,414	0,404	0,421	0,021	0,212	0,217	0,242	0,224	0,016	0,187	0,168	0,173	0,176	0,010
0,459	0,429	0,429	0,439	0,017	0,227	0,271	0,247	0,248	0,022	0,197	0,187	0,192	0,192	0,005
0,483	0,483	0,444	0,470	0,023	0,256	0,286	0,276	0,273	0,015	0,207	0,187	0,197	0,197	0,010
0,493	0,498	0,444	0,478	0,030	0,276	0,296	0,286	0,286	0,010	0,217	0,192	0,207	0,205	0,012
0,503	0,508	0,459	0,490	0,027	0,296	0,311	0,301	0,302	0,008	0,227	0,212	0,217	0,219	0,008
0,518	0,537	0,468	0,508	0,036	0,316	0,325	0,321	0,321	0,005	0,242	0,222	0,227	0,230	0,010
0,523	0,547	0,478	0,516	0,035	0,325	0,335	0,330	0,330	0,005	0,266	0,247	0,242	0,251	0,013
0,547	0,562	0,488	0,533	0,039	0,345	0,340	0,345	0,344	0,003	0,266	0,247	0,251	0,255	0,010
0,547	0,577	0,498	0,541	0,040	0,365	0,350	0,365	0,360	0,009	0,276	0,251	0,266	0,265	0,012
0,552	0,587	0,503	0,547	0,042	0,394	0,365	0,370	0,376	0,016	0,296	0,266	0,276	0,279	0,015
0,567	0,597	0,523	0,562	0,037	0,399	0,375	0,375	0,383	0,014	0,296	0,286	0,291	0,291	0,005
0,572	0,621	0,523	0,572	0,049	0,385	0,360	0,429	0,391	0,035	0,301	0,296	0,301	0,299	0,003

AMOUNT OF METHYLENE BLUE RELEASE FROM BEADS [µg]

APPLE BEADS					MANGO BEADS					COMMERCIAL BEADS				
Sample 1	Sample 2	Sample 3	Mean	S.D.	Sample 1	Sample 2	Sample 3	Mean	S.D.	Sample 1	Sample 2	Sample 3	Mean	S.D.
0,000	0,000	0,000	0,000	0,000	0,000	0,000	0,000	0,000	0,000	0,000	0,000	0,000	0,000	0,000
5,695	5,473	5,399	5,523	0,154	1,479	1,701	1,775	1,652	0,154	1,923	1,775	1,775	1,824	0,085
5,991	5,695	5,399	5,695	0,296	1,775	2,219	2,293	2,096	0,280	2,367	2,145	2,219	2,244	0,113
6,139	5,695	5,547	5,794	0,308	1,849	2,515	2,515	2,293	0,384	2,663	2,367	2,293	2,441	0,196
6,509	6,065	5,843	6,139	0,339	2,367	3,107	3,033	2,835	0,407	2,737	2,441	2,367	2,515	0,196
6,657	6,213	6,065	6,312	0,308	3,180	3,254	3,624	3,353	0,238	2,811	2,515	2,589	2,638	0,154
6,879	6,435	6,435	6,583	0,256	3,402	4,068	3,698	3,723	0,334	2,959	2,811	2,885	2,885	0,074
7,249	7,249	6,657	7,051	0,342	3,846	4,290	4,142	4,093	0,226	3,107	2,811	2,959	2,959	0,148
7,396	7,470	6,657	7,175	0,450	4,142	4,438	4,290	4,290	0,148	3,254	2,885	3,107	3,082	0,186
7,544	7,618	6,879	7,347	0,407	4,438	4,660	4,512	4,536	0,113	3,402	3,180	3,254	3,279	0,113
7,766	8,062	7,027	7,618	0,533	4,734	4,882	4,808	4,808	0,074	3,624	3,328	3,402	3,452	0,154
7,840	8,210	7,175	7,742	0,525	4,882	5,030	4,956	4,956	0,074	3,994	3,698	3,624	3,772	0,196
8,210	8,432	7,322	7,988	0,587	5,178	5,104	5,178	5,153	0,043	3,994	3,698	3,772	3,821	0,154
8,210	8,654	7,470	8,111	0,598	5,473	5,251	5,473	5,399	0,128	4,142	3,772	3,994	3,969	0,186
8,284	8,802	7,544	8,210	0,632	5,917	5,473	5,547	5,646	0,238	4,438	3,994	4,142	4,191	0,226
8,506	8,950	7,840	8,432	0,558	5,991	5,621	5,621	5,745	0,214	4,438	4,290	4,364	4,364	0,074
8,580	9,320	7,840	8,580	0,740	5,769	5,399	6,435	5,868	0,525	4,512	4,438	4,512	4,487	0,043

PERCENTAGE OF METHYLENE BLUE RELEASE FROM BEADS %

Apple beads					Mango beads					Commercial beads				
Sample 1	Sample 2	Sample 3	Mean	S.D.	Sample 1	Sample 2	Sample 3	Mean	S.D.	Sample 1	Sample 2	Sample 3	Mean	S.D.
0,00	0,00	0,00	0,00	0,00	0,00	0,00	0,00	0,00	0,00	0,00	0,00	0,00	0,00	0,00
18,98%	18,24%	18,00%	18,41%	0,51%	4,93%	5,67%	5,92%	5,51%	0,51%	6,41%	5,92%	5,92%	6,08%	0,28%
19,97%	18,98%	18,00%	18,98%	0,99%	5,92%	7,40%	7,64%	6,99%	0,93%	7,89%	7,15%	7,40%	7,48%	0,38%
20,46%	18,98%	18,49%	19,31%	1,03%	6,16%	8,38%	8,38%	7,64%	1,28%	8,88%	7,89%	7,64%	8,14%	0,65%
21,70%	20,22%	19,48%	20,46%	1,13%	7,89%	10,36%	10,11%	9,45%	1,36%	9,12%	8,14%	7,89%	8,38%	0,65%
22,19%	20,71%	20,22%	21,04%	1,03%	10,60%	10,85%	12,08%	11,18%	0,79%	9,37%	8,38%	8,63%	8,79%	0,51%
22,93%	21,45%	21,45%	21,94%	0,85%	11,34%	13,56%	12,33%	12,41%	1,11%	9,86%	9,37%	9,62%	9,62%	0,25%
24,16%	24,16%	22,19%	23,50%	1,14%	12,82%	14,30%	13,81%	13,64%	0,75%	10,36%	9,37%	9,86%	9,86%	0,49%
24,65%	24,90%	22,19%	23,92%	1,50%	13,81%	14,79%	14,30%	14,30%	0,49%	10,85%	9,62%	10,36%	10,27%	0,62%
25,15%	25,39%	22,93%	24,49%	1,36%	14,79%	15,53%	15,04%	15,12%	0,38%	11,34%	10,60%	10,85%	10,93%	0,38%
25,89%	26,87%	23,42%	25,39%	1,78%	15,78%	16,27%	16,03%	16,03%	0,25%	12,08%	11,09%	11,34%	11,51%	0,51%
26,13%	27,37%	23,92%	25,81%	1,75%	16,27%	16,77%	16,52%	16,52%	0,25%	13,31%	12,33%	12,08%	12,57%	0,65%
27,37%	28,11%	24,41%	26,63%	1,96%	17,26%	17,01%	17,26%	17,18%	0,14%	13,31%	12,33%	12,57%	12,74%	0,51%
27,37%	28,85%	24,90%	27,04%	1,99%	18,24%	17,50%	18,24%	18,00%	0,43%	13,81%	12,57%	13,31%	13,23%	0,62%
27,61%	29,34%	25,15%	27,37%	2,11%	19,72%	18,24%	18,49%	18,82%	0,79%	14,79%	13,31%	13,81%	13,97%	0,75%
28,35%	29,83%	26,13%	28,11%	1,86%	19,97%	18,74%	18,74%	19,15%	0,71%	14,79%	14,30%	14,55%	14,55%	0,25%
28,60%	31,07%	26,13%	28,60%	2,47%	19,23%	18,00%	21,45%	19,56%	1,75%	15,04%	14,79%	15,04%	14,96%	0,14%

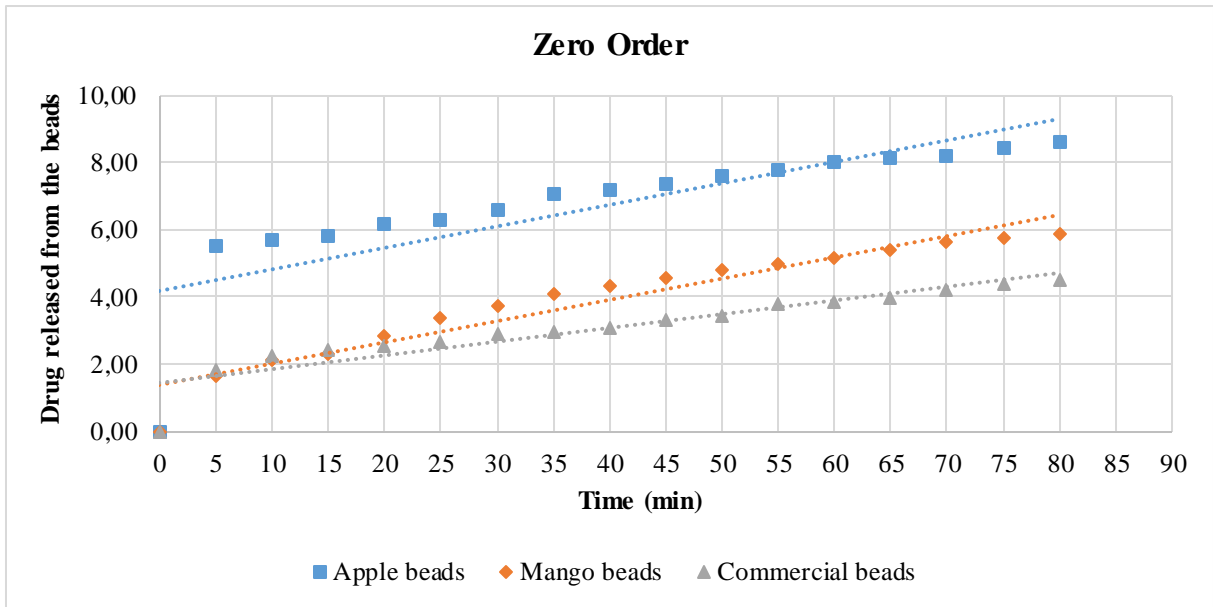


Figure 31: Zero Order drug release model from apple, mango and commercial cellulose

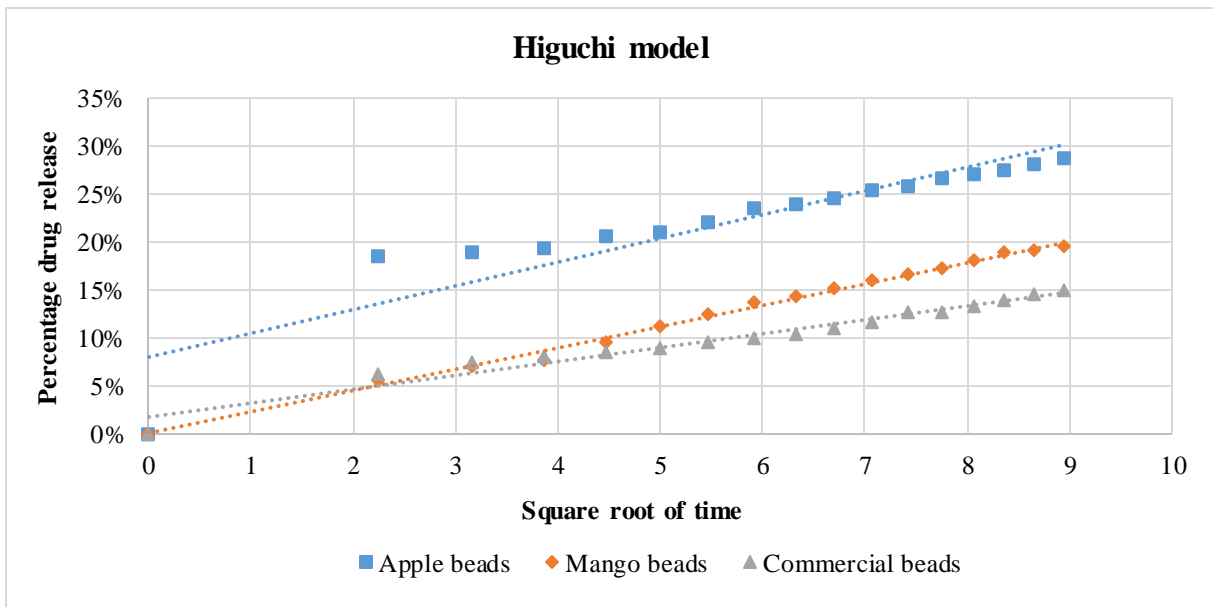


Figure 32: Higuchi model from apple, mango and commercial cellulose

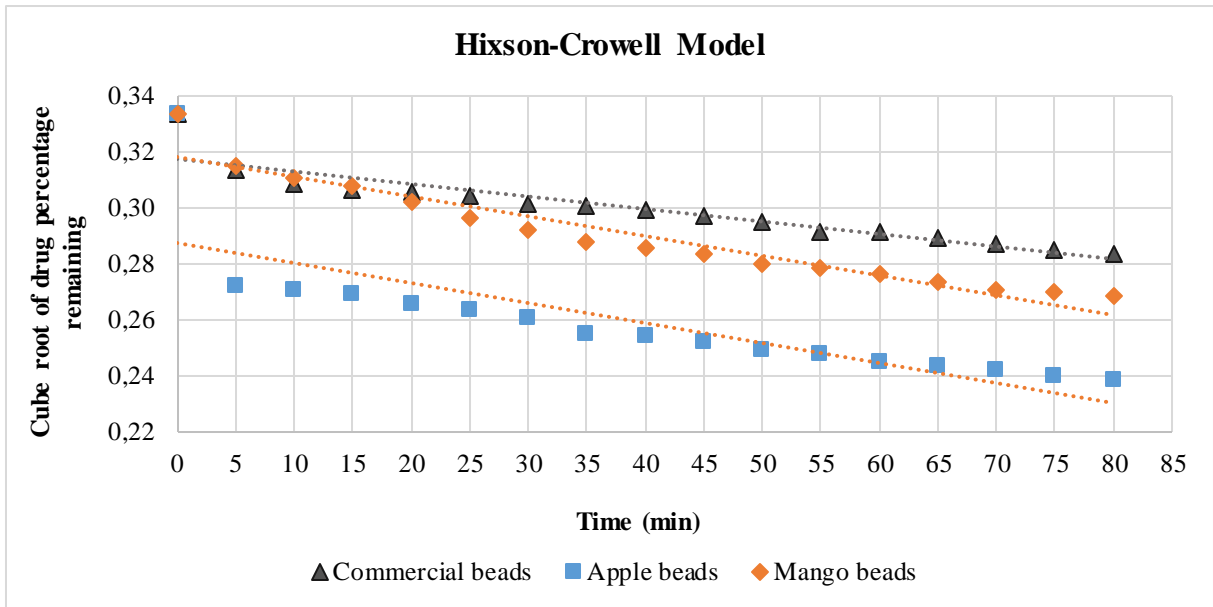


Figure 33: Hixson Model from apple, mango and commercial cellulose

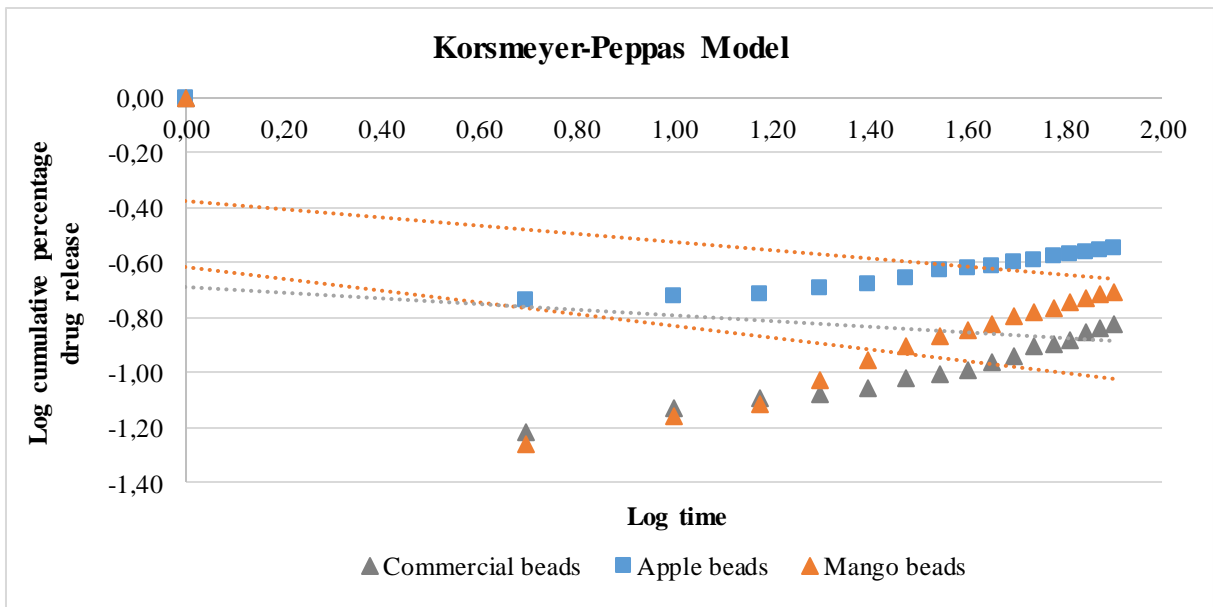


Figure 34: Korsmeyer-Peppas Model from apple, mango and commercial cellulose